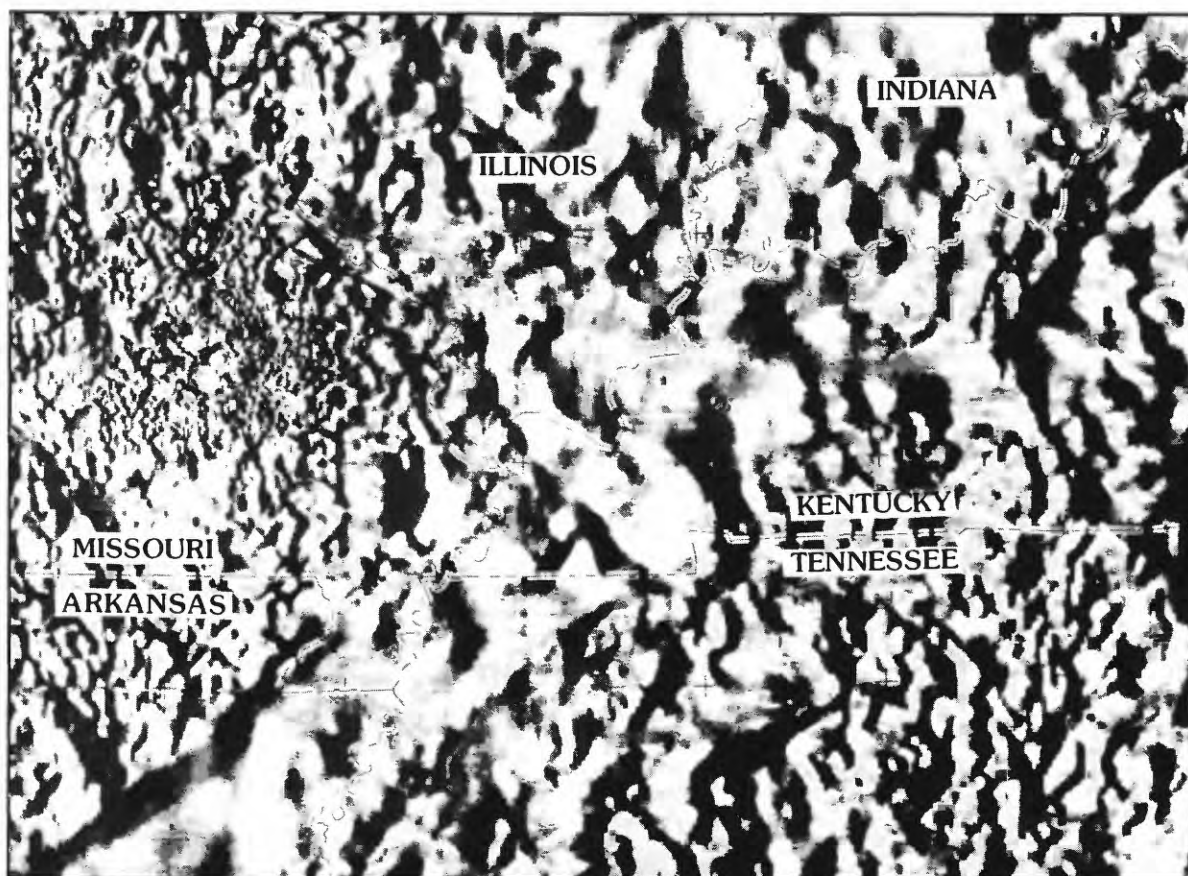# Introduction—Investigations of the New Madrid Seismic Zone

Summary and Discussion of Crustal Stress Data in the Region of the New Madrid Seismic Zone

Preliminary Seismic Reflection Study of Crowley's Ridge, Northeast Arkansas

U.S. GEOLOGICAL SURVEY PROFESSIONAL PAPER 1538–A–C

Cover. Part of a gray, shaded-relief, reduced-to-pole magnetic anomaly map. Map area includes parts of Missouri, Illinois, Indiana, Kentucky, Tennessee, and Arkansas. Illumination is from the west. Figure is from *Geophysical setting of the Reelfoot rift and relations between rift structures and the New Madrid seismic zone*, by Thomas G. Hildenbrand and John D. Hendricks (chapter E in this series).

Investigations of the New Madrid Seismic Zone

Edited by Kaye M. Shedlock *and* Arch C. Johnston

A. Introduction—Investigations of the New Madrid Seismic Zone
    By Kaye M. Shedlock *and* Arch C. Johnston

B. Summary and Discussion of Crustal Stress Data in the Region of the New Madrid Seismic Zone
    By W. L. Ellis

C. Preliminary Seismic Reflection Study of Crowley's Ridge, Northeast Arkansas
    By Roy B. VanArsdale, Robert A. Williams, Eugene S. Schweig III, Kaye M. Shedlock, Lisa R. Kanter, *and* Kenneth W. King

U.S. DEPARTMENT OF THE INTERIOR

BRUCE BABBITT, Secretary

U.S. GEOLOGICAL SURVEY

Robert M. Hirsch, Acting Director

Introduction—Investigations of the New Madrid Seismic Zone

By Kaye M. Shedlock *and* Arch C. Johnston

CONTENTS

FIGURE

INTRODUCTION—INVESTIGATIONS OF THE NEW MADRID SEISMIC ZONE

By Kaye M. Shedlock[1] *and* Arch C. Johnston[2]

The Mississippi Embayment, beginning near the Gulf of Mexico and extending north to the confluence of the Ohio and Mississippi Rivers, is surrounded by the Illinois Basin to the north, the Nashville dome and southern Appalachian Plateau to the east, and the Ouachita and Ozark uplifts to the west. The embayment contains the broad, flat Mississippi River flood plain that is incised into the gently rolling hills of the eastern embayment. Unconsolidated sediments, thin in the north but more than 1 km thick in the south, fill the embayment, an area of rich farmland. The seemingly infinite expanse of bucolic terrain belies the fact that three of the largest known intraplate earthquakes in the world occurred in the northern Mississippi Embayment in a 54-day period during the winter of 1811–12.

Geologically, the embayment is a reentrant into the North American craton that exhibits many subsurface geophysical characteristics of a failed triple junction (Ginzburg and others, 1983). A remnant of a Precambrian upper mantle plume is represented by a relatively high (7.3 km/sec) velocity layer in the lower crust (30–40 km deep). The most prominent buried structure in the northern Mississippi Embayment is the Reelfoot rift, originally defined using magnetic data (Hildenbrand and others, 1982; Hildenbrand and Hendricks, this volume). The Reelfoot rift, about 300 km long and 70 km wide, has 1.6–2.6 km of structural relief on the magnetic basement (fig. 1). The rift is roughly bounded along the northwest side by a series of buried plutons; there is a small buried pluton on the southeast rift margin and a larger pluton buried in the northern end of the rift. The subsurface Blytheville arch, a 10–15-km-wide and 110-km-long zone of arched strata and complex faulting (Hamilton and McKeown, 1988), trends northeast in the center of the rift (fig. 1). The New Madrid seismic zone (NMSZ), a clustered pattern of earthquake epicenters between 5 and 15 km deep, lies mostly within the Reelfoot rift (fig. 1). The NMSZ may be separated geographically into three major trends: a northeast-trending zone from Marked Tree, Ark., to Caruthersville, Mo. (ARK); a north-northwest-trending central zone of earthquakes between Ridgely, Tenn., and New Madrid, Mo. (CEN); and a northeast-trending zone (DWM) from New Madrid to Charleston, Mo. (Himes, and others, 1988). The large 1811–12 New Madrid earthquakes occurred within the NMSZ, although the exact epicenters are unknown and are only inferred from intensity data (fig. 1).

Prior to the 1990's, studies of the Mississippi Embayment and the NMSZ had proceeded largely independent of one another. The Precambrian through early Tertiary (600–30 Ma) formation and evolution of the Reelfoot rift, the Blytheville arch, the plutons, and the embayment were thoroughly mapped and understood to first order. The buried structures, all lying between about 1 km and 6 km deep, and the deformation associated with them tantalizingly overlay the diffusely linear trends of seismicity. By the mid-1980's, a wealth of information and interpretation of the region had been published, most notably U.S. Geological Survey Professional Paper 1236, "Investigations of the New Madrid, Missouri, Earthquake Region" (McKeown and Pakiser, eds., 1982), and U.S. Geological Survey Open-File Report 84–770, "Proceedings of the Symposium on 'The New Madrid Seismic Zone'" (Gori and Hays, eds., 1984). Researchers noted spatial associations between the axial trend of seismicity (between Marked Tree, Ark., and Caruthersville, Mo.) and the Blytheville arch (Zoback and others, 1980; Hamilton and Zoback, 1982; Howe and Thompson, 1984; Crone and others, 1985), as well as the north-northwest-trending central zone of earthquakes and a zone of localized uplift (Russ, 1982). Regional seismic monitoring, begun in 1974, resulted in studies of spatial relationships of earthquake hypocenters and fault-plane solutions that allowed for the interpretation of the ARK and DWM trends as nearly vertical strike-slip zones of faulting (Herrmann and Canas, 1978; Himes and others, 1988). But the physical relationships between the major subsurface structures and the historic and contemporary seismicity remained enigmatic.

Increasing national awareness and concern about the hazards and risks of earthquakes, dramatically emphasized

[1] U.S. Geological Survey, Mail Stop 966, P.O. Box 25046, Denver Federal Center, Lakewood, CO 80225.

[2] Center for Earthquake Research and Information (CERI), Memphis State University, Memphis, TN 38152.

Figure 1. Index map showing the Reelfoot rift, plutons, the Blytheville arch, and epicenters (+) in the New Madrid seismic zone (NMSZ). Epicentral locations for the large 1811–12 earthquakes (circles) are estimated from intensity data. Figure is modified from Luzietti and others (this volume).

by the October 17, 1989, Loma Prieta, Calif., earthquake, led the U.S. Congress to direct the U.S. Geological Survey (USGS) to prepare a plan for intensified study of the NMSZ (Hamilton and Johnston, eds., 1990) and to appropriate

funds to begin implementation of the plan. Thus, in 1990, the NMSZ/Central United States became the first seismically active region east of the Rocky Mountains to be designated a priority research area within the National Earthquake

Hazards Reduction Program (NEHRP). This USGS Professional Paper is a collection of papers presenting the newly intensified research program directed at the NMSZ/Central United States. Major components of this research program are:

- *Tectonic framework studies.*—The integration of geologic and geophysical studies to better understand the tectonic regime of the intraplate NMSZ, to define the geometry of the seismogenic structures in the NMSZ, and to determine the spatial, temporal, and source characteristics of damaging earthquakes in the Central United States.
- *Seismicity and deformation monitoring and modeling.*—The establishment of a modern seismic network in the NMSZ to both monitor the earthquakes and determine the characteristics of the ground motions that they generate, to establish geodetic baselines and continue to monitor crustal deformation in the region, and to model the seismicity and deformation.
- *Improved seismic hazard and risk assessments.*—The delineation of seismic sources, the identification of areas expected to experience strong ground shaking and (or) amplification from earthquakes, the identification of areas subject to ground failure (including liquefaction), and loss-estimation studies.
- *Cooperative hazard mitigation studies.*—The implementation of earthquake-hazard mitigation measures and of preparedness and response programs.

The remainder of this paper briefly describes subsequent chapters of this Professional Paper within the conceptual framework of the revitalized NMSZ/Central United States research program.

TECTONIC FRAMEWORK STUDIES

Mapping of the Reelfoot rift and associated buried structures that was published during the late 1970's and 1980's (Hildenbrand and others, 1977, 1982; Braile and others, 1982a, 1982b) provided the broad tectonic framework of the NMSZ. Additional high-quality potential field, seismic refraction, and seismic reflection data, utilizing a decade of technological advances, have been collected.

Aeromagnetic data collected at lower altitudes and tighter grid spacing provide evidence that suggests the linear seismic trends of the NMSZ follow preferred directions of strain related to intrusions and older faults (Hildenbrand and Hendricks, this volume). Hildenbrand and Hendricks also propose that the Reelfoot rift extends southwest from western Kentucky to east-central Arkansas, where it is abruptly terminated at the Arkansas transform fault.

The northern extent of the Reelfoot rift is controversial. Hildenbrand and Hendricks argue that the rift, a large tectonic system with many related structures including an asymmetric graben, bends eastward and merges with the Rough Creek graben in western Kentucky. Potter and others

(this volume) examine seismic reflection data in the southern Illinois region where the Reelfoot rift and Rough Creek graben may intersect. Potter and others note that the smaller asymmetric graben formation in this region differs from the axially symmetric Reelfoot rift. René and Stanonis (this volume) present shallow reflection seismic profiles of the Wabash Valley fault system in southern Indiana and Illinois, just north of the Rough Creek graben. They interpret listric normal faulting throughout this system, again differing in style of faulting from the Reelfoot rift.

The first magnetotelluric (MT) surveys of the Reelfoot rift reveal an axial resistivity high near the Blytheville arch that may be a previously unrecognized horst (Rodriguez and Stanley, this volume). Gravity data collected over the Mississippi Embayment allow Langenheim (this volume) to infer that faulting in the region is not characterized by major vertical offsets.

Summaries of crustal-stress data in the New Madrid seismic zone (Ellis, this volume) and fluid pressure in the shallow crust (McKeown and Diehl, this volume) provide a wealth of information on the in situ stress and pore pressure in the shallow crust surrounding and overlying the NMSZ.

Five papers use reflection data to examine confirmed or suspected fault systems within the Mississippi Embayment. Both deep and shallow seismic reflection data were collected in the Crittenden County fault zone (CCFZ), a reactivated thrust fault system in the southeastern Reelfoot rift margin. Crone and Pratt (this volume) examine purchased proprietary seismic reflection data and interpret northwest-dipping thrust or oblique-slip faulting in Precambrian through Cretaceous reflectors. Luzietti and others (this volume) use high-resolution Mini-Sosie data to demonstrate that faulting in the CCFZ extends from Cretaceous depths up to at least the Eocene-Quaternary unconformity. Taken together, these papers demonstrate that at least part of the southeastern Reelfoot rift boundary has been active since at least the Cretaceous and may have moved during the Quaternary, in particular during the Holocene.

The Bootheel lineament, first recognized from satellite imagery (Schweig and Marple, 1991), trends north-northeastward for about 135 km between Marked Tree, Ark., and New Madrid, Mo. The surficial morphological expression of the lineament includes linear bodies of liquefied sand, shallow depressions, and small scarps (Schweig and others, this volume). High-resolution Mini-Sosie reflection data collected across this lineament image subtle disruption and gentle warping in Paleozoic through Tertiary layers, interpreted as numerous "flower structures" (Sexton and others, this volume; Schweig and others, this volume). These data are consistent with, but not unambiguously demonstrative of, faulting and deformation in shallow sediments overlying a strike-slip fault.

High-resolution Mini-Sosie seismic reflection data were also collected across the flanks of the most prominent landform in the Mississippi Embayment, Crowley's Ridge (VanArsdale and others, this volume). These data image

ridge-margin faults from Paleozoic through at least Eocene sediments, leading to the interpretation that the topographic relief of Crowley's Ridge may be fault controlled rather than an erosional feature.

SEISMICITY AND DEFORMATION MONITORING AND MODELING

Seismicity in the NMSZ has been monitored since 1974 by the Central Mississippi Valley Seismic Network (CMVSN), sponsored by the USGS and operated originally by Saint Louis University. In the late 1970's, the Nuclear Regulatory Commission joined the USGS as sponsor, and the CMVSN was extended, station density was increased, and Memphis State University joined Saint Louis University as a cooperator. The combined networks consisted of approximately 50 short-period vertical and four 3-component permanent seismograph stations. In 1990, Saint Louis and Memphis State Universities, with USGS sponsorship, began a multiyear effort to upgrade the networks to a single, digital, satellite-telemetered seismic network with at least 40 3-component stations, named the Cooperative New Madrid Seismic Network (CNMSN).

Beginning in October 1989, the 3-component stations of the Portable Array for Numerical Data Acquisition (PANDA) were deployed in the central NMSZ. PANDA station spacing varied between 2 and 27 km, averaging about 12 km overall and about 7 km in the CEN trend of seismicity (Chiu and others, this volume). The PANDA data have resulted in more tightly constrained hypocentral locations and focal mechanisms than are possible with the permanent CNMSN. Using these data, Chiu and others have resolved planar concentrations of hypocenters in the CEN trend that they interpret as southwest-dipping active faults. The surface projections of these inferred faults coincide with the eastern margin of the Lake County uplift (Russ, 1982), providing the first direct relationship between active faulting and surface-deformational features of the NMSZ.

Ellis and others (this volume) evaluate the historical and modern New Madrid region seismic catalog (1800 to 1990) for completeness and annual periodicity. They find no unequivocal evidence of departures from a random distribution of earthquakes at annual periods, suggesting that any modulation of seismic energy release by seasonal influences such as ground water/pore pressure changes is slight to nonexistent.

Gomberg (this volume) employs 2-D boundary-element modeling of strain fields to try to replicate observed surface deformation associated with the 1811–12 earthquakes in order to place limits on the actual faulting process of this sequence. Although many simplifying assumptions are necessary in this modeling technique, Gomberg matches the observed 1811–12 subsidence of Reelfoot Lake and the St. Francis sunklands and the Lake County uplift with just

right-lateral strike-slip motion along the ARK and DWM seismicity trends.

Two studies have begun to address spatial and temporal variation in upper crustal strain rates in the NMSZ. Rates and spatial distribution of strain can be used to infer fault-slip rates and constrain the mechanics of current tectonic deformation. Spatial and temporal strain patterns can be used to assess the earthquake hazard of faults that do not have surface expression. The lack of surface expression of faulting in intraplate regions means that defining active source zones may require a combination of seismic, structural, and geodetic information.

Liu and others (this volume) use Global Position System (GPS) methods to resurvey an existing triangulation network in the southern NMSZ near Caruthersville, Mo. They find a 0.1 μstrain/yr shear-strain rate for the period 1950 to 1990, roughly one-third of the average strain rate in the San Andreas fault system. Visco-elastic modeling of post-1811–12 strain appears to rule out post-1811–12 seismic relaxation as an explanation for this current strain accumulation. Liu and others note that the orientation and sense of shear is consistent with right-lateral strike-slip motion along a buried northeast-trending fault zone.

Snay and others (this volume) combine data from a 1991 GPS survey with pre-existing GPS and triangulation-trilateration data to determine strain rates across the northern NMSZ, near the town of New Madrid, Mo. They find zero strain (at the 95 percent confidence level) across this region, in marked difference to the 0.1 μstrain/yr in the south. Liu and others (this volume) explain this difference as spatial variation due to the finite geometric length and complex seismicity of the NMSZ. Liu and others also note that the strain rate must vary temporally as well, pointing to the lack of cumulative surface expression that would have to exist if the 0.1 μstrain/yr persisted through geologic time.

IMPROVED SEISMIC HAZARD AND RISK ASSESSMENTS

Many of the studies previously discussed, in particular the seismic reflection surveys, the geodetic surveys, and the deformation modeling, also are key contributors to improved seismic hazard and risk assessments. The reflection studies help delineate faults and near-surface structure. The geodetic, deformation, and seismic monitoring studies help determine rates of occurrence of earthquakes and, hence, the rates of occurrence of hazards and risks associated with earthquakes.

Jibson and Keefer (this volume) examine possible trigger mechanisms for landslides along the eastern bluffs of the Mississippi River. They convincingly conclude that most of the currently visible bluff slides were triggered by the 1811–12 earthquakes rather than any anomalous groundwater conditions.

Paleoliquefaction studies (investigations of preserved liquefaction features) provide evidence for the occurrence of large earthquakes and can provide constraints of dates of occurrence and magnitude estimates. Wesnousky and Leffler (this volume) examined drainage ditches in the southern NMSZ. They noted pervasive liquefaction evidence for the 1811–12 earthquakes but no evidence for widespread prehistoric liquefaction events for the previous 5,000 to 10,000 years.

In contrast, Vaughn (this volume) presents data that he interprets as up to four episodes of liquefaction prior to 1811–12 in the lowlands west of Crowley's Ridge. Vaughn cannot differentiate whether local Reelfoot rift (magnitude < 6) or distant NMSZ (magnitude > 7) earthquakes generated the apparent liquefaction. Both of these paleoliquefaction studies establish the need for similar studies throughout the region.

In one of the more intriguing reports of this volume, measurements of seismic attenuation (Q) by Catchings and Mooney indicate that the seismogenic crust in the New Madrid region attenuates seismic energy only about 25 percent as effectively as the crust in the Western United States. Therefore, damaging seismic wave amplitudes will travel much farther in the Central United States. Although this difference in Q is cause enough to worry, it may not be the major contributor to damage in several areas of the Central United States. Amplitude-distance curves show that seismic focusing due to crustal and Moho reflections occur near Memphis, Tenn., and St. Louis, Mo. This focused energy apparently increases seismic amplitudes by more than 1,000 percent over background amplitudes at these sites. This increase in amplitude is roughly equivalent to an increase of at least three Modified Mercalli intensity units. Thus, Memphis and St. Louis will likely experience unusually high amplified ground motions during future large earthquakes.

Equally as important as determining where amplified ground motions are likely to occur is determining what man-made structures may be affected. In a series of maps, developed using new Geographic Information Systems (GIS) technology, Wheeler and others (this volume) present elements of the infrastructure in the Central United States and the seismic hazards associated with them. Their seismotectonic maps include surface faulting, ground shaking, landslides, liquefaction hazards, and deformation. Their infrastructure maps include lifelines, population centers, and critical facilities.

personnel to devise earthquake mitigation and preparedness programs. Olshansky (this volume) examines the potential for State-level seismic-hazard-mitigation policies in those States containing and surrounding the NMSZ. He examines both existing programs and the potential for new seismic-hazard-mitigation programs in seven States. He concludes with an 11-point strategy for State action, including major and minor legislative efforts, for seismic hazard mitigation.

SUMMARY

These Professional Paper chapters provide a wealth of new information about the hazards and risks associated with earthquakes in the NMSZ. The tectonic framework studies have provided a detailed subsurface "snapshot" of the Reelfoot rift and major internal and surrounding structures. For the first time ever in the Central United States, seismologic, deformation, and framework research results are being linked to explain historic and contemporary seismicity. Subsurface planar structures outlined by earthquake hypocenters project to observed surface deformation. The antithetic reactivation of at least one lesser Reelfoot rift boundary fault, through the Tertiary up until possibly as recently as the Holocene, has been unambiguously demonstrated. Near-surface faulting has been imaged along the boundaries of Crowley's Ridge and above the enigmatic Bootheel lineament. Regions of amplified ground motion potential have been mapped.

All of these studies represent significant progress in our ability to accurately assess the seismic hazards and associated risk in the NMSZ and Central United States. But a great deal of work remains to be done. For example, is the Crittenden County fault zone the only reactivated portion of the Reelfoot rift boundary? Is the Bootheel lineament actually a buried fault? What is the relationship between contemporary NMSZ seismicity and the 1811–12 earthquakes? What are the rate and spatial distribution of strain accumulation/relaxation throughout the NMSZ? Are there paleo-indicators that can unambiguously constrain earthquake recurrence and magnitude estimates? All of these questions and more need to be answered in order for us to understand the configuration and seismic potential of the NMSZ. These current studies provide a sound basis for approaching the remaining problems of understanding earthquake hazards and risk in the NMSZ for the 1990's and beyond.

COOPERATIVE HAZARD MITIGATION STUDIES

GIS-based hazard and infrastructure maps (Wheeler and others, this volume) contribute information necessary for city, county, and State planners and emergency-response

REFERENCES CITED

Braile, L.W., Hinze, W.J., Keller, G.R., and Lidiak, E.G., 1982a, The northeastern extension of the New Madrid seismic zone, *in* McKeown, F.A., and Pakiser, L.C., eds., Investigations of the New Madrid, Missouri, Earthquake Region: U.S. Geological Survey Professional Paper 1236, p. 175–184.

Braile, L.W., Keller, G.R., Hinze, W.J., and Lidiak, E.G., 1982b, An ancient rift complex and its relation to contemporary seismicity in the New Madrid seismic zone: Tectonics, v. 1, p. 225–237.

Crone, A.J., McKeown, F.A., Harding, S.T., Hamilton, R.M., Russ, D.P., and Zoback, M.D., 1985, Structure of the New Madrid seismic source zone in southeastern Missouri and northeastern Arkansas: Geology, v. 13, p. 547–550.

Ginzburg, A., Mooney, W.D., Walter, A.W., Lutter, W.J., and Healy, J.H., 1983, Deep structure of the northern Mississippi Embayment: American Association of Petroleum Geophysicists Bulletin, v. 67, no. 11, p. 2031–2046.

Gori, P.L., and Hays, W.W., 1984, Proceedings of the symposium on "The New Madrid seismic zone," O.W. Nuttli, convener and organizer: U.S. Geological Survey Open-File Report 84–770, 468 p.

Hamilton, R.M., and Johnston, A.C., eds., 1990, Tecumseh's Prophecy—Preparing for the next New Madrid earthquake: U.S. Geological Survey Circular 1066, 30 p.

Hamilton, R.M., and McKeown, F.A., 1988, Structure of the Blytheville arch in the New Madrid seismic zone: Seismological Research Letters, v. 59, no. 4, p. 117–121.

Hamilton, R.M., and Zoback, M.D., 1982, Tectonic features of the New Madrid seismic zone from seismic reflection profiles, *in* McKeown, F.A., and Pakiser, L.C., eds., Investigations of the New Madrid, Missouri, Earthquake Region: U.S. Geological Survey Professional Paper 1236, p. 55–82.

Herrmann, R.B., and Canas, J.A., 1978, Focal mechanism studies in the New Madrid seismic zone: Bulletin of the Seismological Society of America, v. 68, p. 1095–1102.

Hildenbrand, T.G., Kane, M.F., and Hendricks, J.D., 1982, Magnetic basement in the upper Mississippi Embayment region— A preliminary report, *in* McKeown, F.A., and Pakiser, L.C., eds., Investigations of the New Madrid, Missouri, Earthquake Region: U.S. Geological Survey Professional Paper 1236, p. 39–53.

Hildenbrand, T.G., Kane, M.F., and Stauder, W., 1977, Magnetic and gravity anomalies in the northern Mississippi Embayment and their spatial relation to seismicity: U.S. Geological Survey Miscellaneous Field Studies Map MF–914, scale 1:1,000,000.

Himes, L., Stauder, W., and Herrmann, R.B., 1988, Indication of active faults in the New Madrid seismic zone from precise location of hypocenters: Seismological Research Letters, v. 59, no. 4, p. 123–131.

Howe, J.R., and Thompson, T.L., 1984, Tectonics, sedimentation, and hydrocarbon potential of the Reelfoot rift: Oil and Gas Journal, Nov. 12, p. 179–190.

McKeown, F.A., Pakiser, L.C., eds., 1982, Investigations of the New Madrid, Missouri, earthquake region: U.S. Geological Survey Professional Paper 1236, 201 p.

Russ, D.P., 1982, Style and significance of surface deformation in the vicinity of New Madrid, Missouri, *in* McKeown, F.A., and Pakiser, L.C., eds., Investigations of the New Madrid, Missouri, Earthquake Region: U.S. Geological Survey Professional Paper 1236, p. 95–114.

Schweig, E.S., III, and Marple, R.T., 1991, The Bootheel lineament—A possible coseismic fault of the great New Madrid earthquakes: Geology, v. 19, p. 1025–1028.

Zoback, M.D., Hamilton, R.M., Crone, A.J., Russ, D.P., McKeown, F.A., and Brockman, S.R., 1980, Recurrent intraplate tectonism in the New Madrid seismic zone: Science, v. 209, p. 971–976.

Summary and Discussion of Crustal Stress Data in the Region of the New Madrid Seismic Zone

By W. L. Ellis

INVESTIGATIONS OF THE NEW MADRID SEISMIC ZONE
Edited by Kaye M. Shedlock *and* Arch C. Johnston

U.S. GEOLOGICAL SURVEY PROFESSIONAL PAPER 1538–B

CONTENTS

FIGURES

TABLES

SUMMARY AND DISCUSSION OF CRUSTAL STRESS DATA IN THE REGION OF THE NEW MADRID SEISMIC ZONE

By W. L. Ellis[1]

ABSTRACT

A compilation of published stress indicators and stress-measurement data from within and near the New Madrid seismic zone (NMSZ) provides some insights into the possible distribution of contemporary crustal stresses in the region. Most of the data are consistent with the east-west to east-northeast–west-southwest direction of maximum horizontal compression that is characteristic of the Midcontinent of the United States, but variations in horizontal stress orientation apparently exist near the left-stepping offset in the linear northeast-southwest trend of the NMSZ. Such variations could indicate a locally complex stress distribution associated with the termination or intersection of seismogenic structures. The data also indicate possible areal variations in stress regime in the region surrounding the NMSZ. In southern Illinois, two strike-slip-faulting and one deeper thrust-faulting earthquake focal-mechanism solutions suggest that the least horizontal stress is about equal to, and sometimes locally exceeds, the vertical stress. This inference is consistent with results of shallow stress measurements and the presence of small north-south-trending thrust faults in coal seams and adjacent strata of Pennsylvanian age in southern Illinois, southwestern Indiana, and western Kentucky. Nearer the NMSZ, focal mechanisms thus far indicate predominantly strike-slip faulting, with the only inferred thrust faulting being along the left-stepping offset in the northeast-trending epicentral alignment. Two normal-faulting focal mechanisms, 125 km northwest of the NMSZ in the St. Francois Mountains area, indicate extensional stress in that region. Areal variations in stress regime could indicate broad crustal deformation such as lithospheric flexure, in which an alternating pattern of compressional and extensional stresses would be expected.

[1] U.S. Geological Survey, Mail Stop 966, P.O. Box 25046, Denver Federal Center, Lakewood, CO 80225.

The published stress data from this region also show that horizontal stress orientations are generally uniform over a wide depth range at many localities. In southern Illinois, shallow stress measurements, borehole breakouts, and earthquake focal mechanisms all provide generally consistent estimates for the maximum horizontal stress direction, suggesting that relatively inexpensive shallow stress measurements might be used to better define the lateral distribution of stress orientations over a broad region surrounding the NMSZ. Mapping of horizontal stress trajectories might contribute to a better understanding of the nature of contemporary crustal deformation and to an evaluation of potential seismic hazards from other faults in the region.

INTRODUCTION

The New Madrid seismic zone, located in the northern Mississippi Embayment (fig. 1), is the site of the great New Madrid earthquakes of 1811–12, the largest earthquakes known to have occurred in the United States east of the Rocky Mountains in historic time. The area remains seismically active and is the focus of ongoing research studies to better understand and define the regional seismic hazard. An improved knowledge of the distribution of crustal stresses in the vicinity of the NMSZ has been identified as an important step to understanding the physical mechanisms responsible for the seismicity of the region (Hamilton and Johnston, 1990). The vertical and lateral distribution of stress magnitudes and areal variations in horizontal stress trajectories may offer clues to the nature of crustal deformation occurring at seismogenic depths, and detailed knowledge of the in situ stresses may be helpful in identifying and evaluating potential seismic hazards from other faults in the region.

Published information regarding crustal stresses in the region of the NMSZ is derived from three types of data: earthquake focal-mechanism solutions, borehole breakouts, and measurements of stress at shallow depths ($\leq$300 m). Most of the available stress data in the region are from the

Figure 1. Map of region around the New Madrid seismic zone showing the distribution of contemporary seismicity, major tectonic features (Braile and others, 1982; McKeown, 1982; Heyl and McKeown, 1978), and the inferred orientation of the maximum horizontal stress, S_H, from all the compiled data (tables 2 and 3). Numbers refer to data entries in tables 2 and 3.

Illinois Basin, about 100–200 km northeast of the NMSZ. A limited amount of stress data are available from within and near the NMSZ and some areas west of the zone. No stress data have been reported from adjacent areas south and east of the zone. The quantity and spatial extent of stress data in the New Madrid region is insufficient to fully characterize the lateral distribution of crustal stresses in and around the NMSZ. The fact that in situ stresses can be variable on a variety of scales also introduces uncertainties into any attempts at interpretation or comparative analyses of the sparse data. It is important to recognize, however, that variability in stress fields, no matter the scale, arises mainly

from mechanical and structural heterogeneities in the Earth. Efforts to better characterize trends in stress distributions may therefore lead to an improved understanding of the mechanics and seismotectonics of intraplate seismic source zones. Although sparse for purposes of interpretation, the available data from around the NMSZ are more abundant than at most Eastern U.S. seismic source zones, and the data do provide some tentative insights into the distribution of contemporary stresses in the region.

The objective of this paper is to compile in one source the currently available published information concerning crustal stresses within a 200-km distance of the NMSZ. Previous compilations of stress data and stress indicators from the NMSZ region (Zoback and Zoback, 1980, 1989; Nelson and Bauer, 1987; Hamburger and Rupp, 1988) either do not focus on the NMSZ in detail or do not contain all published information currently available. Consequently, some information and data relevant to crustal stress evaluations of this region are scattered among various publications, some of which receive limited distribution. Stress data from a relatively large region around the NMSZ is of potential interest because the zone of most active seismicity extends for a linear distance of about 200 km along the northeast-trending Reelfoot rift, a late Precambrian–early Paleozoic rift that underlies the northern Mississippi Embayment (fig. 1). Variations in regional stresses due to this zone of apparent major crustal weakness might extend for considerable distances away from the zone. Also, the 200-km range encompasses several regionally significant faults and fault zones adjacent to the NMSZ that may have an effect on, or be within the influence of, the stress distribution from this large tectonic feature.

TYPES OF DATA

FOCAL MECHANISMS

The P- and T-axis orientations from single-event earthquake focal-mechanism solutions in the New Madrid region are used to infer the approximate orientation of the maximum horizontal compressive stress, S_H. The reliability of principal stress directions inferred from earthquake focal-mechanism solutions has been discussed in the literature (McKenzie, 1969; Raleigh and others, 1972; Zoback and Zoback, 1980; Michael, 1987). In the general case of an earthquake on a preexisting fault, the P-axis may differ by as much as 35°–40° from the maximum principal stress direction (Raleigh and others, 1972; Zoback and Zoback, 1980). The orientation of S_H inferred from any single focal mechanism provides only an approximation of the true horizontal stress orientation, especially when the fault plane is unknown. Experience has shown, however, that the average P- and T-axis orientations from earthquakes in a given area

generally correspond very well with stress directions inferred from other stress indicators or stress measurements (Zoback and Zoback, 1980).

A total of 18 published, single-event, earthquake focal-mechanism solutions (Stauder and Nuttli, 1970; Herrmann and Canas, 1978; Herrmann, 1979; Taylor and others, 1989; Schweig and others, 1991) are compiled for the NMSZ region. In addition, a composite mechanism from the main shock and aftershocks from the magnitude 4.5 New Hamburg, Mo., earthquake of September 16, 1990, is included (Stauder and others, 1990). Most of these focal-mechanism solutions are from earthquakes located within or near the NMSZ and the Wabash Valley seismic zone in southern Illinois, where most of the larger earthquakes in this region have occurred. The hypocentral depth range represented by these focal-mechanism solutions is from 1.5 to 22 km, with most of the events in the 8–16-km depth range.

Single-event and composite focal-mechanism solutions from microearthquakes within the left-stepping offset in the northeasterly trend in seismicity in the central part of the NMSZ have been reported (O'Connell and others, 1982; Nicholson and others, 1984; Andrews and Mooney, 1985). The variability in P- and T-axis orientations and inferred mode of faulting indicated by these focal-mechanism data suggests a complex distribution of stresses within the small central portion of the NMSZ. Because focal-mechanism solutions from microearthquakes are more likely to reflect small-scale stress variations, and because the central left-stepping zone is small compared to the much larger region of study, these microearthquake focal-mechanism data are not included in this compilation. The stress distribution within the relatively small left-stepping zone of seismicity is therefore likely to be more complex than indicated from this compilation of P-axis orientations from the larger magnitude, single-event earthquake data.

BOREHOLE BREAKOUTS

Experience has shown that borehole breakouts, or stress-induced spalling of borehole walls, is a generally reliable indicator of horizontal stress direction (Bell and Gough, 1979; Plumb and Hickman, 1985; Plumb and Cox, 1987). Laboratory and theoretical studies have confirmed that borehole breakouts can result from shear failure due to the concentration of far-field stresses at the borehole wall and that the orientation of breakouts reflects the orientation of the least stress normal to the hole axis (Haimson and Herrick, 1985; Zheng and others, 1989). Careful interpretation of wellbore logs to establish the existence and orientation of stress-induced breakouts can yield valuable information regarding horizontal stress trajectories. Breakouts in 16 different boreholes in the NMSZ region have been reported (Dart, 1985; Dart and Zoback, 1989). Most of these data are from boreholes located in the southern part of the Illinois

Table 1. Quality-ranking criteria for data in tables 2 and 3.

[Adapted from quality-ranking system for stress orientations of Zoback and Zoback (1991); M, magnitude; s.d., standard deviation]

Data-quality rank	Ranking criteria
Focal mechanism	
A	Average P-axis or formal inversion of four or more single-event solutions in close geographic proximity. At least one event M ≥ 4.0; other events M ≥ 3.0.
B	Well-constrained single-event solution (M ≥ 4.5) or average of two well-constrained, single-event solutions (M ≥ 3.5) determined from first motions and other methods (e.g., moment tensor waveform modeling or inversion).
C	Single-event solution (constrained by first motions only, often based on author's quality assignment). M ≥ 2.5. Average of several well-constrained composites (M ≥ 2.0).
D	Single composite solution. Poorly constrained single-event solution. Single-event solution for event with M < 2.5.
Wellbore breakout	
A	Ten or more distinct breakout zones in a single well with s.d. ≤ 12° and (or) combined length > 300 m. Average of breakouts in two or more wells in close geographic proximity with combined length > 300 m and s.d. ≤ 12°.
B	At least six distinct breakout zones in a single well with s.d. ≤ 20° and (or) combined length > 100 m.
C	At least four distinct breakouts with s.d. ≤ 25° and (or) combined length > 30 m.
D	Less than four consistently oriented breakouts or < 30 m combined length in a single well. Breakouts in a single well with s.d. ≥ 25°.
Hydraulic fracture	
A	Four or more hydrofrac orientations in single well with s.d. ≤ 12°; depth > 300 m. Average of hydrofrac orientations for two or more wells in close geographic proximity, s.d. ≤ 12°.
B	Three or more hydrofrac orientations in a single well with s.d. < 20°.
C	Hydrofrac orientations in a single well with 20° < s.d. < 25°; distinct hydrofrac orientation change with depth; deepest measurements assumed valid. One or two hydrofrac orientations in a single well.
D	Single hydrofrac measurement at < 100 m depth.
Overcore	
A	Average of consistent (s.d. ≤ 12°) measurements in two or more boreholes extending more that two excavation radii from the excavation wall and far from any known local disturbances; depth > 300 m.
B	Multiple, consistent (s.d. < 20°) measurements in one or more boreholes extending more than two excavation radii from excavation wall; depth > 100 m.
C	Average of multiple measurements made near surface (depth > 5–10 m) at two or more localities in close proximity with s.d. ≤ 25°. Multiple measurements at depth > 100 m with 20° < s.d. < 25°.
D	All near-surface measurements with s.d. > 15°; depth < 5 m. All single measurements at depth. Multiple measurements at depth with s.d. > 25°.

Basin, but breakout orientations from one borehole within and one borehole southwest of the NMSZ, in northeastern Arkansas (Dart and Swolfs, 1991), are included in the compilation. The depth range represented by the breakout orientation data is 0.1–2.2 km.

SHALLOW STRESS MEASUREMENTS

The results of shallow stress measurements have been reported for eight locations within 200 km of the NMSZ. Haimson (1974) conducted hydraulic fracturing measurements in south-central Illinois, and Aggson and Hooker (1982), in a summary of U.S. Bureau of Mines overcoring stress measurements made in the United States, included horizontal stress components determined at two locations in southeastern Missouri. It is noted that one of the overcoring stress measurements in Missouri was conducted in an underground mine at a site of locally complex geology. The horizontal stress orientations derived from this measurement deviate significantly from the regional trend and may reflect a locally complex stress field (J.R. Aggson, oral commun., 1991). In a more recent study of thrust faulting in southern Illinois, Nelson and Bauer (1987) included some previously unpublished stress estimates obtained by strain-gage measurements in boreholes and strain relaxation measurements

Table 2. Maximum horizontal stress azimuths inferred from earthquake focal-mechanism data in the region of the New Madrid seismic zone.

Data index number (State)	Magnitude	Date	Depth (km)	Inferred stress regime[a]	Inferred $S_{H_{max}}$ azimuth	Data used[b]	Quality[c]	References (see footnote)
1 (Mo.)	4.3	2/2/62	7.5	SS	N. 31° E.	P&SW	C	1, 3, 4
2 (Mo.)	4.8	3/3/63	15.0	SS	N. 14° W.	P&SW	C	1
3 (Ill.)	3.8	8/14/65	1.5	SS	N. 59° E.	P&SW	C	1, 2
4 (Mo.)	4.9	10/21/65	5.0	N	N. 66° E.	P&SW	B	1, 4
5 (Mo.)	4.3	7/21/67	15.0	N	N. 41° W.	P&SW	C	1
6 (Ill.)	5.5	11/9/68	22.0	T	N. 83° W.	P&SW	B	1, 2, 4, 5
7 (Ark.)	4.4	11/17/70	16.0	SS	N. 86° E.	P&SW	C	1, 3, 4
8 (Ill.)	4.7	4/3/74	15.0	SS	N. 83° E.	P&SW	C	1, 2
9 (Mo.)	4.2	6/13/75	9.0	SS	N. 43° E.	P&SW	C	1, 3, 4
10 (Ark.)[d]	5.0	3/25/76	12.0	SS	N. 87° E.	P&SW	B	1, 3, 4
	4.5		16.0					
11 (Ill.)	4.9	6/10/87	10.0	SS	N. 89° E.	P&SW	B	2
12 (Ark.)[e]	≤4.5	post 1982	3.0–6.0	SS	N. 50° E.	?	?	6
13 (Mo.)	4.5	9/26/90	13.9	SS	N. 64° E	P&WM	B	7
14 (Mo.)	4.6	5/4/91	7.1	SS	N. 45° E.	P	C	8
15 (Tenn.)	3.8	8/29/90	13.9	SS	N. 88° E.	P	C	7

References: 1, Herrmann (1979); 2, Taylor and others (1989); 3, Herrmann and Canas (1978); 4, Zoback and Zoback (1980); 5, Stauder and Nuttli (1970); 6, Schweig and others (1991); 7, Stauder and others (1990); 8, Chiu and others (1991).

[a] SS, predominantly strike-slip faulting; T, predominantly thrust faulting; N, predominantly normal faulting.

[b] P&SW, p-wave first arrivals and surface-wave data; P&WM, p-wave first arrivals and surface-wave modeling; P, p-wave first arrivals only.

[c] Quality ranking A through D using criteria of Zoback and Zoback (1991). See table 1.

[d] Average P-axis azimuth from two earthquakes with very similar focal mechanisms.

[e] Average P-axis azimuth from four earthquakes with similar focal mechanisms.

on core samples from three locations in southern Illinois. Well-documented and internally consistent sets of stress data obtained by the U.S. Bureau of Mines overcoring technique have been reported from recent measurements in two coal mines in southern Illinois (Ingram and Molinda, 1988). The depth range of the shallow stress measurements compiled in the NMSZ region is approximately 1.5–300 m.

DATA QUALITY

The quality ranking system for stress-orientation data that was developed and published by Zoback and Zoback (1989, 1991) is applied here to provide an estimate of the reliability with which the data are thought to represent the tectonic stress. The question of assigning a measure of quality to stress-determination results or to data used to infer some property of the stress field is, by nature, subjective. Methods of data collection, analysis, and reporting vary from author to author, and the results of different studies may be supported by varying quantities and coherence of input data. In many cases, the original data upon which a result is reported is often not published, and it is therefore necessary to rely on the author's judgment of quality.

The quality-ranking method of Zoback and Zoback has been developed over a number of years. The method

attempts to indicate both the reliability of the data, as gaged by its quantity, extent, and internal consistency, and the degree to which it is believed to be an indicator of tectonic stress, as judged by the volume of rock represented by the stress indicator and its depth in the crust. This method does not guarantee that all available data that may serve as reliable indicators of regional tectonic stress are included or that poor indicators are eliminated. It does, however, provide a reasonable approach to filtering widely disparate types of published stress data and stress indicators such that the potential significance of each can be judged. Table 1 presents a part of the Zoback and Zoback (1989, 1991) quality-ranking system appropriate to the data summarized here for the NMSZ.

DATA SUMMARY

A summary of the currently available stress data in the NMSZ region is shown in table 2, as inferred from earthquake focal-mechanism data, and in table 3, as inferred from borehole-breakout data and determined from shallow stress measurements. Figure 1 is a map of the NMSZ region showing the distribution of seismicity, major tectonic features, and inferred S_H orientation for all of the data listed in tables 2 and 3, and figure 2 is the same map showing S_H orientations as inferred from only data of quality A and B (see

Table 3. Summary of stress determination and borehole-breakout data in the region of the New Madrid seismic zone.

[Leaders (--) indicate no data available]

Index number and State	Depth (km)	Stress magnitudes (MPa)	S_{Hmax} azimuth	Data-quality estimate[a]	References (see footnote)
Borehole-breakout measurements					
16 (Ill.)	0.1–0.4	--	N. 57° E.	B	1
17 (Ill.)	0.8–1.1	--	N. 65° E.	B	1
18 (Ky.)	0.5–0.9	--	N. 88° W.	A	1
19 (Ill.)	0.8–1.5	--	N. 86° E.	B	1
20 (Ky.)	0.2–0.7	--	N. 87° W.	A	1
21 (Ill.)	0.3–0.8	--	N. 78° W.	B	1
22 (Ill.)	1.4–2.2	--	N. 67° E.	B	1
23 (Ind.)	0.5–0.7	--	N. 88° E.	B	1
24 (Ill.)	0.8–0.9	--	N. 50° E.	B	1
25 (Ind.)	0.5–0.8	--	N. 81° W.	B	1
26 (Ill.)	0.9–1.3	--	N. 35° E.	B	1
27 (Ill.)	0.7–0.9	--	N. 74° E.	B	1
28 (Ill.)	0.8–0.9	--	N. 90° E.	D	1
29 (Ill.)	0.5–0.6	--	N. 86° E.	D	1
30 (Ark.)	1.3–2.9	--	N. 73° E.	A	2, 8, 9
31 (Ark.)	1.3–2.9	--	N. 75° E.	A	2, 8, 9
Hydraulic-fracture measurements					
32 (Ill.)	0.1	$S_{vert} = 2.2$ $S_{Hmax} = 7.8$ $S_{Hmin} = 2.4$	N. 62° E.	B	3, 7
Stress-relief, overcore, and strain-gage measurements					
33 (Ill.)	≤ 0.3	--	N. 67° W.	NA	4
34 (Ill.)	≤ 0.3	$S_{vert} = 5.3$ $S_{Hmax} = 22.0$ $S_{Hmin} = 9.6$	N. 76° E.	NA	4
35 (Ill.)	≤ 0.3	--	N. 87° E.	NA	4
36 (Ill.)	0.3	$S_{vert} = 6.1$ $S_{Hmax} = 9.7$ $S_{Hmin} = 5.5$	N. 88° E.	B	5
37 (Ill.)	0.2	$S_{vert.} = 3.6$ $S_{Hmax} = 10.3$ $S_{Hmin} = 3.5$	N. 78° E.	B	5
38 (Mo.)	surface	$S_{Hmax} = 22.0$ $S_{Hmin} = 9.6$	N. 77° E.	D	6, 10
39 (Mo.)[b]	0.3	$S_{Hmax} = 25.4$ $S_{Hmin} = 11.0$	N. 17° W.	D	6, 10

References: 1, Dart (1985); 2, Dart and Swolfs (1991); 3, Haimson (1974); 4, Nelson and Bauer (1987); 5, Ingram and Molinda (1988); 6, Aggson and Hooker (1982); 7, Zoback and Zoback (1980); 8, Dart (1987); 9, Dart and Zoback (1989); 10, Hooker and Johnson (1969).

[a] Quality ranking A through D using criteria of Zoback and Zoback 1991 (see table 1). NA indicates data type not included in Zoback and Zoback quality-ranking scheme or insufficient information available.

[b] Possible local stress anomaly at geologically complex site (J.R. Aggson, oral commun., 1991).

table 1). Figure 3 is a map of the region showing the compiled focal-mechanism solutions plotted at their approximate epicentral locations. The S_H orientations and focal-mechanism plots shown in figures 1, 2, and 3 are indexed by number to the data points listed in tables 2 and 3.

It is noted that data entry no. 10 in table 2 is the average of very similar focal-mechanism solutions from two earthquakes that occurred at the same epicentral location. These two earthquakes had hypocentral depths of 12 km and 16 km, respectively, and were separated in time by 20
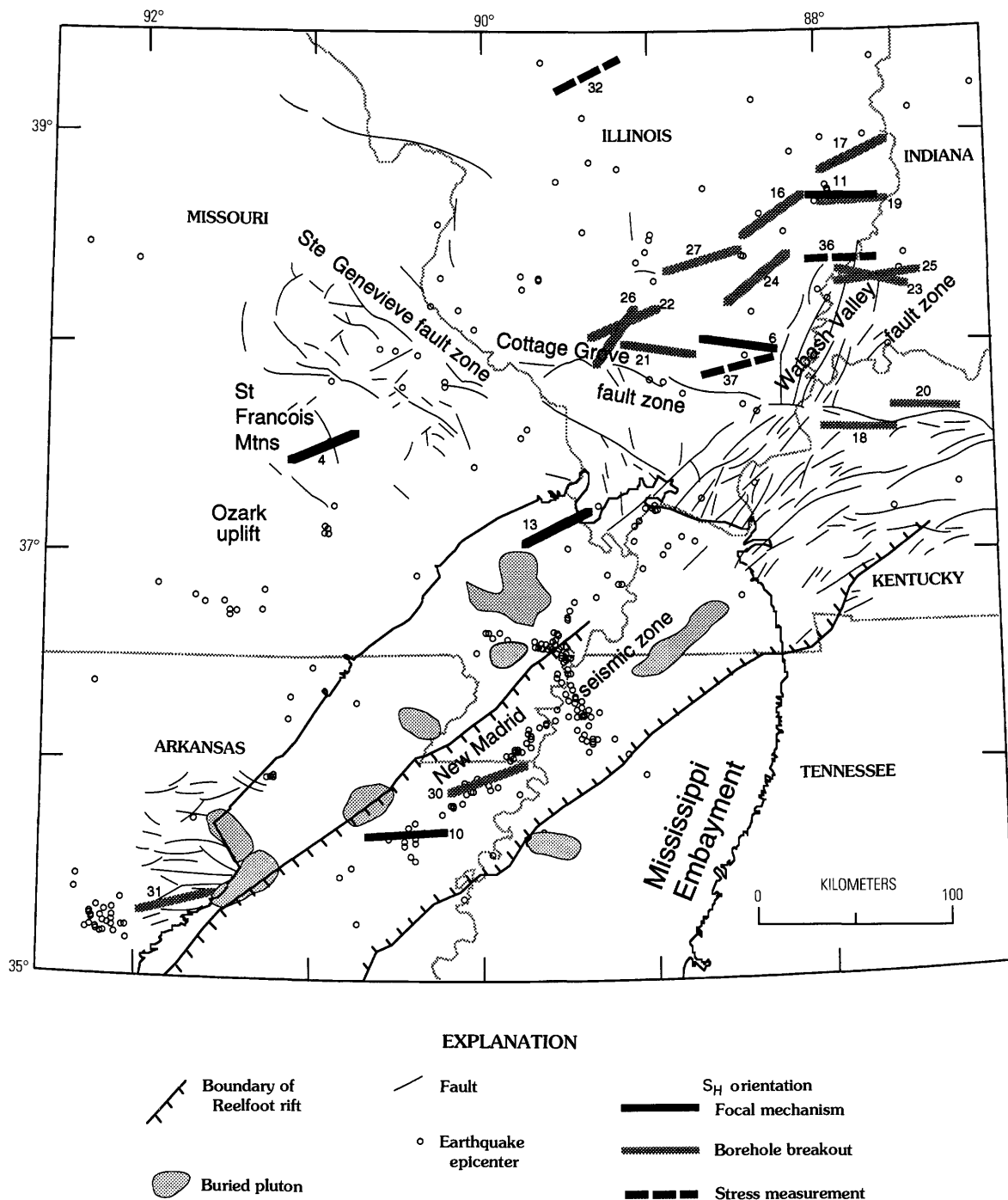
Figure 2. Map of region around the New Madrid seismic zone showing the distribution of contemporary seismicity, major tectonic features (Braile and others, 1982; McKeown, 1982; Heyl and McKeown, 1978), and the inferred orientation of the maximum horizontal stress, S_H, from the compiled A- and B-quality data (tables 2 and 3). Numbers refer to data entries in tables 2 and 3.

minutes (Herrmann and Canas, 1978; Herrmann, 1979). Also, data entry no. 12 is the average of nearly identical focal-mechanism solutions from four closely grouped earthquakes that occurred between depths of 3 and 6 km in the Enola, Ark., earthquake swarm (Schweig and others, 1991).

DISCUSSION

STRESS DIRECTIONS

The data from stress indicators and shallow stress measurements in the NMSZ region are generally consistent with
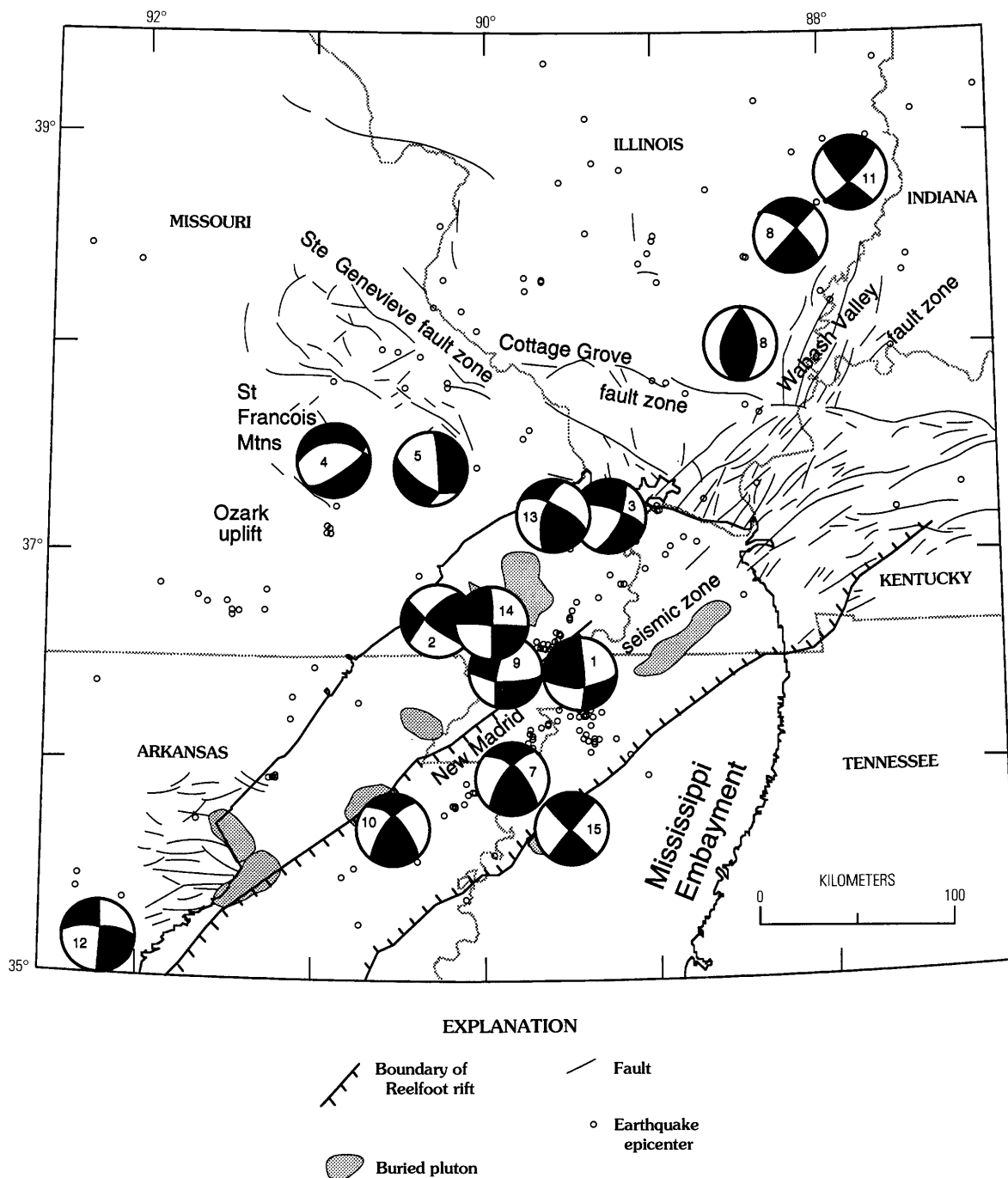
Figure 3. Map of region around the New Madrid seismic zone showing compiled earthquake focal-mechanism diagrams listed in table 2 and plotted at their approximate epicentral locations. Compressional quadrants in the focal-mechanism diagrams are shaded. Numbers refer to data entries in table 2.

the east-west to northeast-southwest direction of maximum horizontal compression that is characteristic of the Midcontinent of the United States (Zoback and Zoback, 1980, 1989). Figure 4 is a plot of the S_H orientations inferred from this data compilation and shows the semicircular vector means (Agterberg, 1974) for each data type. The semicircular vector mean directions of S_H for all of the data is N. 80° E.

Local variations in the regional stress orientations may be present, however, near some tectonic and structural features. Indications of such potential variations in stress orientation come primarily from the focal-mechanism data, which unfortunately may be the least accurate indicator of stress directions. It is therefore not clear whether the observed variations in P- and T-axis orientations represent actual

changes in stress orientations or whether they simply result from uncertainty in how well the P- and T-axes correspond with the principal stress directions. The observation, however, that stress directions inferred from focal mechanisms in this region in most cases agree quite well with other nearby stress indicators (fig. 1) of different types increases confidence that significant departures from the regional trend in P-axis orientation for any single focal-mechanism solution may indicate a true local stress variation. Also, the most pronounced change in P-axis directions in the NMSZ region are near the left-stepping offset in the northeasterly alignment of earthquake epicenters in the central part of the NMSZ (fig. 1), an area where a complex distribution of stresses might be expected.

The earthquake focal-mechanism data that indicate a possible rotation in stress direction near the left-stepping offset in seismicity (data points 1, 2, 9, and 14 in fig. 1) are rated C quality, and no A- and B-quality data are available from this area. Also, the map of A- and B-quality data (fig. 2) shows a more consistent orientation of S_H azimuth for the region than when the C-quality data are included (fig. 1). This observation raises the question that perhaps the apparent stress rotation is not real and is only a consequence of less reliable, and possibly less accurate, data. Although this possibility cannot be dismissed, there are reasons to believe that the focal mechanisms in the area likely do reflect an actual change in stress direction. First, all four focal-mechanism solutions within the area indicate a northward rotation of S_H azimuth relative to the regional trend. Second, one of the mechanisms (data point 14, fig. 1) is from a recent earthquake that was surrounded and recorded by a modern regional seismic network and a local network of three-component, high-dynamic-range seismometers, providing a robust data set for analysis of the event (Chiu and others, 1991). The C quality assigned to this data is because of the fact that the mechanism was determined from first-motion data only (table 1).

In actuality, the quality of the data from this particular area is likely to be more reliable than indicated by the quality-ranking criteria in table 1. The agreement in P-axis orientation between the recent earthquake and focal-mechanism solutions from the earlier earthquakes that occurred prior to installation of the local network and before the current level of understanding of the velocity structure in the region reinforces the reliability of the earlier data. Also, two of the earlier earthquakes (data points 1 and 9, fig. 1) are ranked C quality only because their magnitudes of 4.3 and 4.2, respectively, are slightly less than the magnitude 4.5 cutoff for B-quality data (table 1). Thus, the focal-mechanism data that indicate a possible rotation in stress direction near the left-stepping offset in seismicity in the central part of the NMSZ may actually be of better quality than implied by the quality-ranking scheme. It is noteworthy that the average P-axis orientation from these four data points would also
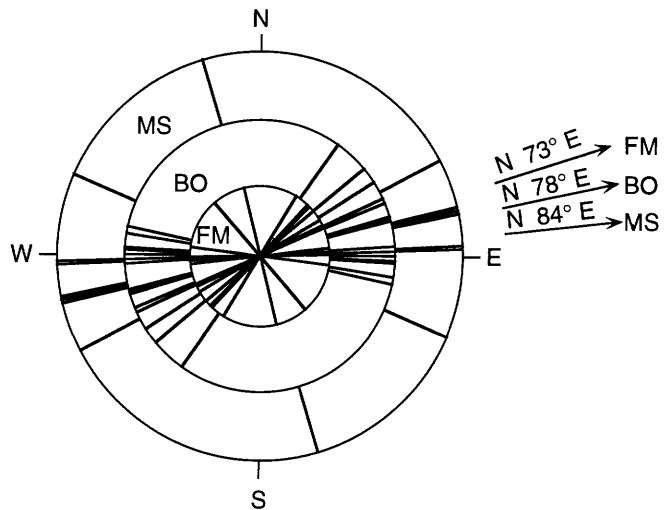

Figure 4. Plot of maximum horizontal stress orientations as inferred from the three data types in tables 2 and 3. FM, focal mechanisms; BO, borehole breakouts; MS, shallow stress measurements. Arrows indicate the semicircular vector mean of orientations for each data type.

indicate a northward rotation of S_H azimuth, and this average orientation would rank as an A-quality data point using the widely accepted criteria of table 1. Thus, although the individual data points from near the left-stepping offset in seismicity are only ranked as C quality, they may actually be more reliable than indicated, and, taken together, they may provide a strong indication of a local and perhaps significant variation in the regional stress trend.

A notable variation from the regional trend in horizontal stress directions is also indicated by focal-mechanism solutions in the St. Francois Mountains area of southeast Missouri. There, the inferred S_H directions from two focal-mechanism solutions from earthquakes about 50 km apart differ by nearly 90°. Both of these mechanisms, one of which is ranked C quality, also indicate normal-faulting stress conditions, in contrast to the predominantly strike-slip and thrust-faulting mechanisms for other earthquakes in the region. The difference in S_H orientations inferred from these two focal mechanisms could be interpreted as indicating that the horizontal stress components in this area are approximately equal to each other, but less than the vertical stress, with the result that normal faulting on preexisting faults with a wide range of strikes is possible. The two shallow stress measurements in this same area also give opposing results for the S_H direction (fig. 1), but, as noted earlier, the one measurement result that contrasts with the regional trend in stress orientation may reflect a localized stress variation associated with complex geologic structure at the measurement site. Both shallow stress measurements, however, indicate horizontal stress magnitudes that greatly exceed the vertical stress, contrary to the stress state indicated by the deeper normal-faulting focal mechanisms.

STRESS REGIMES

The types of earthquake focal mechanisms and their distribution (fig. 3) suggest the possibility of broad areal variations of stress regime in the region around the NMSZ. In the Illinois Basin, north of the Mississippi Embayment, the mixture of one thrust-faulting and two strike-slip-faulting focal mechanisms implies that the stress field there could be transitional between strike-slip and thrust faulting, wherein the least horizontal stress is about equal to and locally exceeds the vertical stress. This possibility is consistent with the existence of minor thrust faults in shallow coal seams and adjacent strata of Pennsylvanian age in southern Illinois, southwestern Indiana, and western Kentucky (Nelson and Bauer, 1987). These thrust faults, which formed in response to an approximately east-west-directed maximum horizontal compression, cannot be precisely dated, but because no known past tectonic stress field or nontectonic process was found to have produced them, Nelson and Bauer (1987) believe that they formed in response to the contemporary tectonic stress field. The shallow stress measurements in southern Illinois (table 3) also indicate that the contemporary stress regime within the upper few hundred meters is transitional between thrust-faulting and strike-slip faulting, with the maximum horizontal stress aligned in a generally east-west direction. Whether this transitional stress regime in the Illinois Basin is confined only to shallow depths is uncertain, but the presence of at least one deep thrust-faulting earthquake suggests the possibility that it may exist throughout the upper several kilometers of crust.

To the south of the Illinois Basin, focal-mechanism solutions from earthquakes in and near the most active part of the NMSZ indicate that the predominant component of fault movement there is strike-slip. The only indications of earthquakes with a predominantly thrust-faulting component of displacement in this area come from focal-mechanism solutions from microearthquakes in the vicinity of the left-stepping offset in seismicity in the central part of the NMSZ (O'Connell and others, 1982; Nicholson and others, 1984; Andrews and Mooney, 1985). As noted earlier, this area also produces some normal-faulting and strike-slip-faulting composite focal mechanisms and is probably an area of complex stress distribution associated with the intersection of seismically active structures.

Southwest of the NMSZ, in northeastern Arkansas, focal-mechanism solutions from four earthquakes in the tightly clustered Enola, Ark., earthquake swarm (only the average focal mechanism is shown on fig. 3) are interpreted as representing strike-slip movement on east-west-trending faults (Schweig and others, 1991). Herrmann (1979) reported a thrust-faulting focal mechanism with a northwesterly oriented P-axis for an earthquake that occurred approximately 60 km to the southwest of this earthquake swarm (outside the area included in this compilation). The apparent absence of thrust-faulting stress conditions in and

immediately around the most active part of the NMSZ (with the exception of the small area within the central left-stepping offset) suggests that the least horizontal-stress in the areas near the seismic zone may be somewhat reduced in magnitude relative to the area to the north and possibly to the south. Conversely, the prevailing stress regime throughout the above areas could be strike slip, with the thrust-fault focal mechanisms only representing very local stress anomalies and with the high lateral stresses in the Illinois Basin confined to the near-surface.

As noted earlier, the two focal-mechanism solutions from earthquakes located in the St. Francois Mountains area of southeastern Missouri both indicate normal-faulting stress conditions (Herrmann, 1979), a highly unusual circumstance for the Midcontinent. These normal-faulting mechanisms imply that an extensional stress regime may exist in the Ozark uplift northwest of the NMSZ, although the areal extent of such a stress regime cannot be defined with the limited data available. The shallow stress measurements made in this same area indicate that large-magnitude horizontal stresses are present near the surface, suggesting that the stress regime varies with depth in this area (from one of thrust faulting near the surface to normal faulting at seismogenic depths).

Although sparse, the focal-mechanism data suggest the possibility of lateral variations in stress regime in the NMSZ region. A transitional stress regime between thrust and strike-slip faulting may be present in southern Illinois; a predominantly strike-slip stress regime may exist in the area immediately around the NMSZ; and an extensional stress regime may exist at depth in the area of the Ozark uplift in southeast Missouri. Such areal variations in stress regime, should they prove to be real, could result from broad-scale geologic or tectonic features. Lateral variations in crustal strength and density contrasts in the crust could give rise to broad-scale variations in regional stress. Lithospheric flexure, perhaps resulting from sediment loading or lateral density contrasts in the lower crust, could also result in broad areal variations in stress regime. Crustal flexure, if present, would be expected to produce alternating patterns of compression and extension over large areas that would be superimposed upon the regional stresses thought to originate from plate-driving forces. Because the largest flexural stresses would develop near the outer margins of the flexing elastic plate, their influences would be more pronounced at relatively shallow depths. Such a conceptual model has been proposed by Dewey (1988) as a possible explanation for seismicity exterior to former rift basins in intraplate settings.

If, on the other hand, the most active part of the NMSZ simply represents a narrow zone of crustal weakness within a relatively uniform regional stress, then there should be some evidence of redistribution of the regional stresses around the weakened core zone. Maximum horizontal stress orientations in the Illinois Basin, north of the NMSZ, do tend to align in a more east-west orientation than is typical for

most of the midcontinent region. Insufficient data in other areas surrounding the NMSZ, however, make it unclear whether this change in orientation may be related to the NMSZ or whether it represents a general change to a more east-west orientation of the maximum horizontal stress trajectories in the central Midcontinent. More data on stress orientation and relative stress magnitudes are needed to adequately characterize the details and spatial extent of the stress distribution around the NMSZ.

STRESS DISTRIBUTION WITH DEPTH

The distribution of horizontal stress orientations in the region of the NMSZ shows little apparent variation with depth. The semicircular vector-mean directions of S_H for each of the three data types, which correspond generally with depth, differ only by a maximum of 11° (fig. 4). Figure 5 is a plot of the S_H azimuths as a function of depth for the compiled data. Note that the scatter in orientations of S_H for the shallow stress measurements is comparable to that inferred from the intermediate-depth borehole breakouts and the deeper focal-mechanism solutions. The similar means and range in orientations for each of the three sets of data implies approximately equal uncertainty in the reliability of data from each set to reflect the mean S_H direction. This observation also suggests that a carefully planned and implemented program of shallow stress measurements may offer a viable means of mapping the horizontal stress orientations in a wide region surrounding the NMSZ. The level of precision in horizontal-stress trajectories determined from shallow stress measurements may be comparable to that of borehole-breakout orientations, and it is probably better than for horizontal-stress trajectories determined from earthquake focal-mechanism P-axis orientations. It is noted, however, that relative stress magnitudes determined from shallow stress measurements may not be indicative of those at depth. The lateral distribution of shallow stress magnitudes could, however, be useful as a possible indicator of crustal flexure and for distinguishing between various seismotectonic models for the NMSZ region.

SUMMARY

A compilation of shallow stress measurements and deeper stress indicators in the region of the NMSZ shows that, whereas most of the horizontal-stress trajectories are consistent with the east-west to east-northeast–west-southwest direction of maximum horizontal compression characteristic of the midcontinent region, local variations in stress directions apparently exist. These variations may be related to tectonic structures and the intersections of seismically active fault zones. Earthquake focal-mechanism solutions also suggest areal variations in the stress regime that could possibly be indicative of the type of broad crustal deformation occurring in the region. Unfortunately, the available
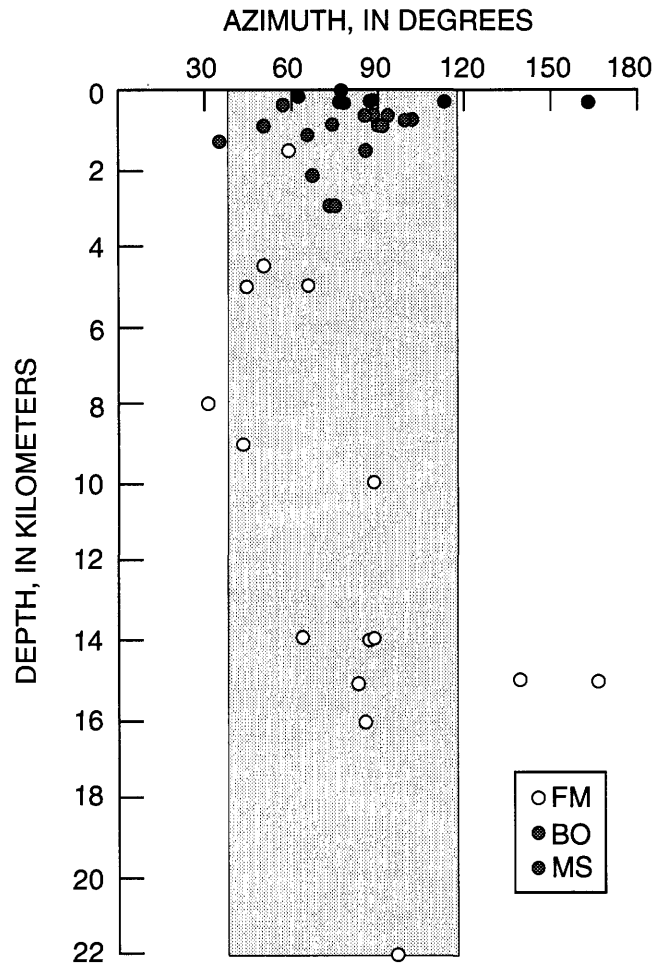

Figure 5. Maximum horizontal stress azimuth as a function of depth for the data in tables 2 and 3, distinguished by data type. FM, focal mechanisms; BO, borehole breakouts; MS, shallow stress measurements. Shaded area represents range of ±40° of the semicircular vector mean of N. 80° E. for all of the data. This range is an estimate of the uncertainty in how well the P-axis orientation from any single focal-mechanism diagram corresponds to the maximum compressive stress direction (Raleigh and others, 1972) when the actual fault plane is unknown.

database of stress measurements and stress indicators is not of sufficient quantity or lateral extent to adequately define the stress distribution in the region of the NMSZ or to firmly establish relationships between stress, structure, and seismicity. Additional stress data are needed, especially to the west and east of the NMSZ. A better characterization of the stress distribution, in association with the results of geodetic strain determinations and deformation modeling studies, should lead to an improved understanding of the seismotectonics of the region. The consistency between horizontal stress directions derived from the various types of data over a wide range of depths suggests the possibility that shallow stress measurements may offer a viable and economic means of contributing to an improved understanding of contemporary stresses in the NMSZ region.

REFERENCES CITED

Aggson, J.R., and Hooker, V.E., 1982, In-situ rock stress determination: Techniques and applications, in Underground Mining Methods Handbook: New York, Society of Mining Engineers of American Institute of Mining, Metallurgical, and Petroleum Engineers, p. 1498-1505.

Agterberg, F.P., 1974, Geomathematics: Amsterdam, Elsevier, 596 p.

Andrews, M.C., and Mooney, W.D., 1985, The relocation of microearthquakes in the northern Mississippi Embayment: Journal of Geophysical Research, v. 90, p. 10223–10236.

Bell, J.S., and Gough, D.I., 1979, Northeast-southwest compressive stress in Alberta: Evidence from oil wells: Earth and Planetary Science Letters, v. 45, p. 475–482.

Braile, L.W., Hinze, W.J., Keller, G.R., and Lidiak, E.G., 1982, The northeastern extension of the New Madrid seismic zone, in McKeown, F.A., and Pakiser, L.C., eds., Investigations of the New Madrid, Missouri, Earthquake Region: U.S. Geological Survey Professional Paper 1236, p. 175–184.

Chiu, S.C., Hwang, H., Chiu, J.M., and Johnston, A.C., 1991, The Risco, Missouri earthquake, May 4, 1991, in Program, Abstracts, and Minutes of the 63rd Annual Meeting, Eastern Section, Seismological Society of America: Seismological Research Letters, v. 62, nos. 3–4, p. 151–199.

Dart, R., 1985, Horizontal-stress directions in the Denver and Illinois Basins from the orientation of borehole breakouts: U.S. Geological Survey Open-File Report 85–733, 41 p.

———1987, South-central United States well-bore breakout-data catalog: U.S. Geological Survey Open-File Report 87-405, 95 p.

Dart, R.L., and Swolfs, H.S., 1991, Contemporary stress in northeastern Arkansas [abs.]: Transactions of the American Geophysical Union (EOS), v. 72, no. 17, p. 264.

Dart, R.L., and Zoback, M.L., 1989, Wellbore breakout stress analysis within the central and eastern continental United States: The Log Analyst Journal, v. 30, no. 1, p. 12–25.

Dewey, J.W., 1988, Midplate seismicity exterior to former rift-basins: Seismological Research Letters, v. 59, p. 213–218.

Haimson, B.C., 1974, A simple method for estimating in situ stresses at great depths, in Field Testing and Instrumentation of Rock: American Society for Testing of Materials STP 554, p. 156–182.

Haimson, B.C., and Herrick, C.G., 1985, In situ stress evaluation from borehole breakouts, experimental studies, in Research and Engineering Applications in Rock Masses—Symposium on Rock Mechanics, [26th, Rapid City, S. Dak.]: Rotterdam, A.A. Balkema, p. 1207–1218.

Hamburger, M.W., and Rupp, J.A., 1988, The June 1987 southeastern Illinois earthquake: Possible tectonism associated with the La Salle anticlinal belt: Seismological Research Letters, v. 59, p. 151–157.

Hamilton, R.M., and Johnston, A.C., eds., 1990, Tecumseh's prophecy: Preparing for the next New Madrid earthquake: U.S. Geological Survey Circular 1066, 30 p.

Herrmann, R.B., 1979, Surface wave focal mechanisms for eastern North American earthquakes with tectonic implications: Journal of Geophysical Research, v. 84, p. 3543–3552.

Herrmann, R.B., and Canas, J.A., 1978, Focal mechanism studies in the New Madrid seismic zone: Bulletin of the Seismological Society of America, v. 68, p. 1095–1102.

Heyl, A.V., and McKeown, F.A., 1978, Preliminary seismotectonic map of central Mississippi Valley and environs: U.S. Geological Survey Miscellaneous Field Studies Map MF–1011, scale 1:250,000.

Hooker, V.E., and Johnson, C.F., 1969, Near-surface horizontal stresses including the effects of rock anisotropy: U.S. Bureau of Mines Report of Investigations 7224, 29 p.

Ingram, D.K., and Molinda, G.M., 1988, Relationship between horizontal stresses and geologic anomalies in two coal mines in southern Illinois: U.S. Bureau of Mines Report of Investigations 9189, 18 p.

McKenzie, D.P., 1969, The relationship between fault plane solutions for earthquakes and the directions of the principal stresses: Bulletin of the Seismological Society of America, v. 59, p. 591–601.

McKeown, F.A., 1982, Overview and discussion, in McKeown, F.A., and Pakiser, L.C., eds., Investigations of the New Madrid, Missouri, Earthquake Region: U.S. Geological Survey Professional Paper 1236, p. 1–4.

Michael, A.J., 1987, Use of focal mechanisms to determine stress—A control study: Journal of Geophysical Research, v. 92, p. 357–368.

Nelson, W.J., and Bauer, R.A., 1987, Thrust faults in the Illinois Basin—Result of contemporary stress?: Geological Society of America Bulletin, v. 98, p. 302–307.

Nicholson, C., Simpson, D.W., Singh, S., and Zollweg, J.E., 1984, Crustal studies, velocity inversions, and fault tectonics; results from a microearthquake survey in the New Madrid seismic zone: Journal of Geophysical Research, v. 89, p. 4545–4558.

O'Connell, D.R., Bufe, C.G., and Zoback, M.D., 1982, Microearthquakes and faulting in the area of the New Madrid, Missouri–Reelfoot Lake, Tennessee, in McKeown, F.A., and Pakiser, L.C., eds., Investigations of the New Madrid, Missouri, Earthquake Region: U.S. Geological Survey Professional Paper 1236, p. 31–38.

Plumb, R.A., and Cox, J.W., 1987, Stress directions in eastern North America determined to 4.5 km from borehole elongation measurements: Journal of Geophysical Research, v. 92, p. 4805–4816.

Plumb, R.A., and Hickman, S.H., 1985, Stress-induced borehole elongation—A comparison between the four-arm dipmeter and borehole televiewer in the Auburn geothermal well: Journal of Geophysical Research, v. 90, p. 5513–5521.

Raleigh, C.B., Healy, J.H., and Bredehoeft, J.D., 1972, Faulting and crustal stress at Rangely, Colorado, in Flow and Fracture of Rocks: American Geophysical Union Geophysical Monograph 16, p. 275–284.

Schweig, E.S., VanArsdale, R.B., and Burroughs, R.K., 1991, Subsurface structure in the vicinity of an intraplate earthquake swarm, central Arkansas: Tectonophysics, v. 186, p. 107-114.

Stauder, W.J., Herrmann, R., Wuenscher, M., Taylor, K., Mitchel, S., and Whittington, M., 1990, Central Mississippi Valley earthquake bulletin: Saint Louis University, Quarterly Bulletin No. 65, third quarter 1990.

Stauder, W.J., and Nuttli, O.W., 1970, Seismic studies: south central Illinois earthquake of November 9, 1968: Bulletin of the Seismological Society of America, v. 60, p. 973–981.

Taylor, K.B., Herrmann, R.B., Hamburger, M.W., Pavlis, G.L., Johnston, A., Langer, C., and Lam, C., 1989, The southeastern Illinois earthquake of 10 June 1987: Seismological Research Letters, v. 60, p. 101–110.

Zheng, Z., Kemeny, J., and Cook, N.G., 1989, Analysis of borehole breakouts: Journal of Geophysical Research, v. 94, p. 7171–7182.

Zoback, M.D., and Zoback, M.L., 1991, Tectonic stress field of North America and relative plate motions, in Slemmons, D.B., Engdahl, E.R., Zoback, M.D., and Blackwell, D.D., eds., Neo-tectonics of North America: Boulder, Colorado, Geological Society of America, Decade Map, v.1, p. 339–366.

Zoback, M.L., and Zoback, M.D., 1980, State of stress in the con-terminous United States: Journal of Geophysical Research, v. 85, p. 6113–6156.

Zoback, M.L., and Zoback, M.D., 1989, Tectonic stress field of the continental United States, in Pakiser, L.C., and Mooney, W.D., eds., Geophysical Framework of the Continental United States: Boulder, Colorado, Geological Society of America Memoir 172, p. 523–539.

Preliminary Seismic Reflection Study of Crowley's Ridge, Northeast Arkansas

By Roy B. VanArsdale, Robert A. Williams, Eugene S. Schweig III, Kaye M. Shedlock, Lisa R. Kanter, *and* Kenneth W. King

INVESTIGATIONS OF THE NEW MADRID SEISMIC ZONE
Edited by Kaye M. Shedlock *and* Arch C. Johnston

U.S. GEOLOGICAL SURVEY PROFESSIONAL PAPER 1538–C

CONTENTS

FIGURES

TABLES

PRELIMINARY SEISMIC REFLECTION STUDY OF CROWLEY'S RIDGE, NORTHEAST ARKANSAS

By Roy B. VanArsdale,[1] Robert A. Williams,[2] Eugene S. Schweig III,[3]
Kaye M. Shedlock,[2] Lisa R. Kanter,[4] *and* Kenneth W. King[2]

ABSTRACT

Five high-resolution seismic reflection lines (24-channel Mini-Sosie data with 1-s record length) were acquired across the margins of Crowley's Ridge in northeast Arkansas to test the hypothesis that Crowley's Ridge is fault bounded. Three of the lines traversed the margins of the northern segment of the ridge near Jonesboro, Ark., and the other two were located south of Jonesboro, across the margins of the southern segment. Subsurface faulting of Paleozoic strata through the Eocene Wilcox Group was interpreted in the lines beneath the ridge margins at all five sites. The data did not resolve the uppermost 0.15 s (150 m) of two-way travel time, so it is not possible to determine if the Pliocene-Pleistocene sediments have been faulted. Thus, we can not determine if the ridge truly owes its topographic relief to fault displacement or if Tertiary faulting controlled subsequent Quaternary river incision. However, at one site, the ridge margin is interpreted as a fault scarp because the ridge height is the same as the structural relief on the ridge-bounding fault and fault displacement can be traced into the shallowest reflectors (0.15 s).

The Mini-Sosie data reveal a rather complex Tertiary structural history. Paleocene and possible early Eocene faulting is evident in thickened Midway Group and lower Wilcox Group strata across some faults. Post-Wilcox (early Eocene) faulting is present in all of the lines, and post-Claiborne Group (middle Eocene) folding and faulting are suggested in some of the lines. The steepness of the faults and the normal and reverse displacements occurring within a

small area and over a relatively short length of time suggests that these faults may be the upper portions of strike-slip flower structures.

INTRODUCTION

Crowley's Ridge, in northeast Arkansas (fig. 1), has been interpreted to be an erosional remnant formed during Quaternary incision of the ancestral Mississippi and Ohio Rivers (Call, 1889; Stephenson and Crider, 1916; Fisk, 1944; Guccione and others, 1986). However, the Reelfoot rift COCORP line (AR-6 of Nelson and Zhang, 1991) has revealed a down-to-the-west fault beneath the western margin of the southern segment of the ridge. The pronounced linearity and declivity of the ridge margins throughout its length suggests that the ridge may also be fault bounded at other locations.

Crowley's Ridge consists of two discrete segments with geomorphic characteristics that further suggest the ridge is structurally controlled. At lat 35°45'N., Crowley's Ridge abruptly changes width, geology, bearing, and symmetry (Cox, 1988a) (fig. 1). North of lat 35°45'N., the axis of the northern ridge segment is straight, bearing N. 30° E., whereas south of this latitude, the southern ridge segment is straight and trends N. 5° E. The northern segment is asymmetrical in transverse profile, having a steep west margin relative to the southern segment (Cox, 1988a). Drainage-basin analyses of streams on the two segments suggest that the northern segment has undergone southeast tilting during the Quaternary (Cox, 1988a).

The geomorphology of Crowley's Ridge and the interpreted fault beneath the western margin of the southern ridge segment suggest that the entire ridge may be bounded by faults. In order to test the hypothesis that Crowley's Ridge has been structurally uplifted, we collected a total of 12 km of high-resolution seismic reflection data (Mini-Sosie) at five locations across the ridge margins (fig. 1).

[1] Department of Geology, University of Arkansas, Fayetteville, AR 72701.

[2] U.S. Geological Survey, Mail Stop 966, P.O. Box 25046, Denver Federal Center, Lakewood, CO 80225.

[3] U.S. Geological Survey, Center for Earthquake Research and Information (CERI), Memphis State University, Memphis, TN 38152.

[4] Center for Earthquake Research and Information (CERI), Memphis State University, Memphis, TN 38152.

Figure 1.   Map of northeast Arkansas (modified from Cox, 1988a). Dashed lines represent margins of the Reelfoot rift (Hildenbrand and others, 1982). Numbered lines (1–5) are Mini-Sosie lines. Lower case letters are petroleum exploration wells: q, Quintin Little No. 1 Little; n, J.F. Scott Trustees No. 2-A Nelson; h, Henley-Lanagren Co. No. 1 E.E. Hogue; j, C.E. Walters and others No. 1 H. Johnson; t, Tennark Inc. R.M. Martin and others; m, Volcanic Oil and Gas Co. No. 1-A McDaniel; f, W. Adams No. 1 Fee; s, Houston Mineral and Oil No. 1 Singer. P, Paragould; J, Jonesboro; H, Harrisburg; MT, Marked Tree; M, Memphis.

GEOLOGIC SETTING

SURFACE GEOLOGY OF CROWLEY'S RIDGE AND VICINITY

Crowley's Ridge is a 320-km-long topographic ridge that extends from Thebes, Ill., to Helena, Ark. (Arkansas portion shown in fig. 1). The ridge is from 1.6 to 19 km wide, averages 60 m above the adjacent lowlands, and is stratigraphically composed of Eocene and Pliocene-Pleistocene unconsolidated sediments (fig. 2). The Eocene sequence is dominated by continental and deltaic sands and clays with minor intervals of lignite (Murray, 1961). Eocene units dip approximately 0.5° southeast (Meissner, 1984) and are unconformably overlain by Pliocene-Pleistocene fluvial sands, gravels, and clays that locally exceed 50 m in thickness (Holbrook, 1980). These Pliocene-Pleistocene fluvial deposits have been correlated with the Citronelle (Lafayette) Formation of the Gulf Coast (Potter, 1955; Saucier, 1974; Guccione and others, 1986). Above these fluvial deposits, up to 10 m of Pleistocene loess is locally preserved with major accumulation confined to the southern portion of Crowley's Ridge (Saucier, 1974; Guccione and others, 1986; Autin and others, 1991).
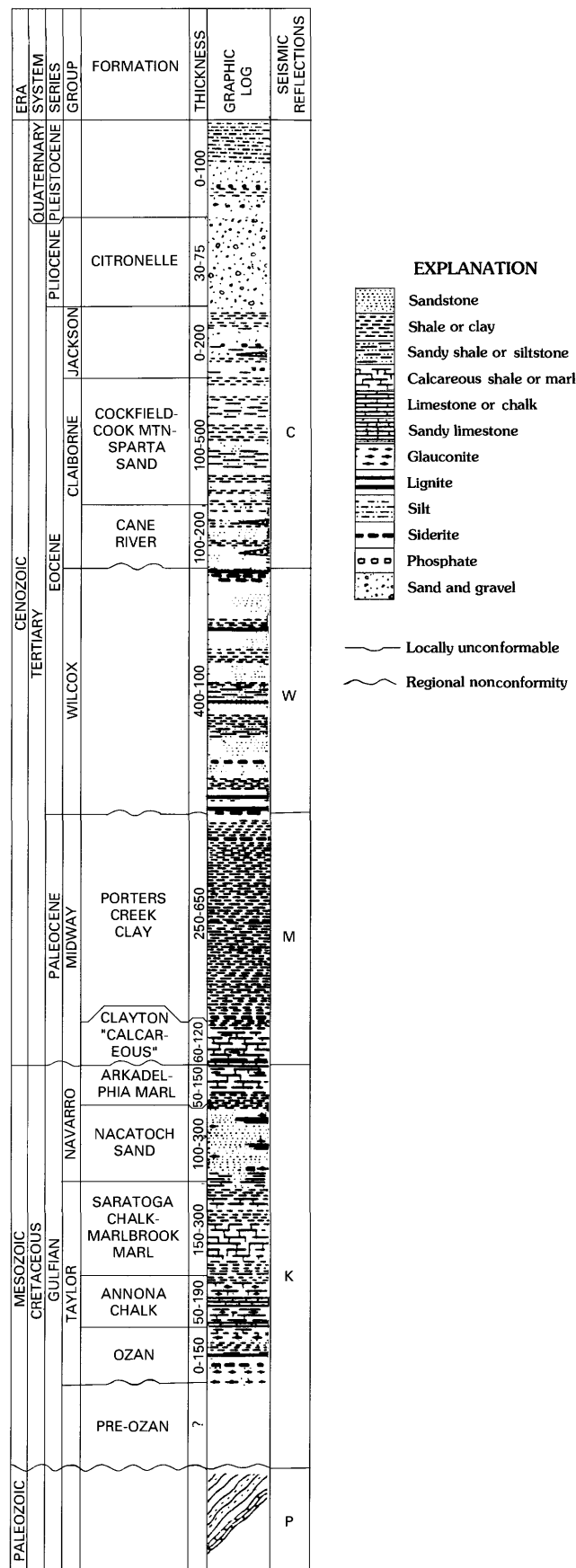
Flanking the ridge at our reflection-line sites is an early Wisconsin braided-stream terrace that is 80,000 to 35,000 years old (Royall and others, 1991). This terrace level is underlain by glacial outwash and valley-train deposits of the Mississippi and Ohio Rivers; the terrace is capped by loess (Saucier, 1974; Rutledge and others, 1990).

GEOLOGIC HISTORY OF THE MISSISSIPPI EMBAYMENT

Crowley's Ridge lies within the northwestern portion of the Mississippi Embayment, a broad and gentle south-south-west-plunging syncline of Cretaceous and Tertiary age (Stearns, 1957; Stearns and Marcher, 1962). In order to better understand the structural setting of Crowley's Ridge, we herein briefly review the structural history of the Mississippi Embayment area.

Drill hole data and exposures in the Ozarks of southeastern Missouri indicate that, during late Precambrian time, the upper Mississippi Embayment area was a subaerial landscape with from 150 to 450 m of topographic relief (Schwalb, 1982; Buschbach and Schwalb, 1984) cut into Middle Proterozoic granites and rhyolites (Bickford, 1988).

EXPLANATION

Sandstone
Shale or clay
Sandy shale or siltstone
Calcareous shale or marl
Limestone or chalk
Sandy limestone
Glauconite
Lignite
Silt
Siderite
Phosphate
Sand and gravel

Locally unconformable
Regional nonconformity

Figure 2 (facing column). Cretaceous-Quaternary stratigraphic section for northeast Arkansas with principal seismic reflectors (modified from Renfroe, 1949). P, Paleozoic; K, Cretaceous; M, Midway Group; W, Wilcox Group; C, Claiborne Group.

This landscape was dramatically altered by the initiation of the northeast-trending Reelfoot rift in late Precambrian or Early Cambrian time (Ervin and McGinnis, 1975; Kane and others, 1981; Hildenbrand and others, 1982). The Reelfoot rift underlies and is essentially coincident with the present Mississippi Embayment syncline (Ervin and McGinnis, 1975). Middle Ordovician through Early Devonian unconformities mark marine transgressions and regressions that may have been accompanied by reactivation of rift-bounding faults. Late Devonian deformation resulted in Upper Devonian black shales lying with angular unconformity over strata as old as Ordovician. Uplift of the Pascola arch in the upper embayment area, between late Paleozoic and middle Cretaceous time, ultimately resulted in the erosion of most of the Paleozoic section to as deep as Cambrian Lamotte Sandstone strata across the arch (Stearns, 1957; Stearns and Marcher, 1962). Beneath Crowley's Ridge at Jonesboro, Upper Cretaceous sedimentary rocks overlie Ordovician carbonates (Caplan, 1954).

Formation of the Mississippi Embayment initiated in Late Cretaceous time with subsidence and deposition of Upper Cretaceous marine sediments (Stearns, 1957; Pryor, 1960) and intrusion of plutons along the rift-bounding faults. The axis of the embayment is nearly coincident with the underlying Reelfoot rift and appears to reflect Cretaceous reactivation of the ancient rift (Braile and others, 1982). Embayment subsidence continued into early Tertiary time, as reflected in Paleocene to middle Eocene marine and terrestrial sedimentary rocks (Stearns, 1957). Late Eocene compression resulted in minor faulting and folding within the embayment (Howe and Thompson, 1984; Luzietti and others, 1992). Absence of Oligocene and Miocene strata suggests that, during this time, the embayment area was subaerially exposed. In Pliocene time, the embayment underwent terrestrial deposition as reflected in the Pliocene-Pleistocene fluvial gravels preserved in Crowley's Ridge and the embayment perimeter (Potter, 1955). The Pleistocene was dominated by erosion of most of the Pliocene-Pleistocene section, deposition of glacial outwash and loess, and the establishment of the current drainage system within the embayment. Sedimentation and tectonism within the Mississippi Embayment continues to the present with Mississippi River sedimentation and the New Madrid seismicity (Nuttli, 1973, 1982; Johnston, 1982; Braile and others, 1982).

SEISMICITY AND NEOTECTONICS OF CROWLEY'S RIDGE AND VICINITY

Current seismicity in the Mississippi Embayment primarily occurs east of Crowley's Ridge and is coincident with structural highs within the Reelfoot rift (fig. 3). Specifically, the northeast-trending Blytheville arch and the northwest-trending Lake County uplift are the most seismically active areas in the embayment (Russ, 1979, 1982; Hamilton and

Zoback, 1982; Crone and others, 1985; Hamilton and McKeown, 1988; McKeown and others, 1990). Although the area has fewer events than the Blytheville arch and Lake County uplift areas, there is also seismicity along the eastern margin of the rift north of Memphis, Tenn. (fig. 3). This eastern-rift-margin seismicity is of interest because of the recent identification of Eocene and probable post-Eocene deformation along the Crittenden County fault, located 10 km west of Memphis (Luzietti and others, 1992).

Crowley's Ridge overlies and crosses the western margin of the Reelfoot rift near Jonesboro, Ark. (fig. 1). The intersection area of the ridge and the western margin of the rift also coincides with the Jonesboro pluton, the change from northern to southern ridge segments, and a proposed northwest-trending fault line (Fisk, 1944; Krinitzsky, 1950; O'Leary and Hildenbrand, 1978; Cox, 1988a, 1988b). One of the most striking geomorphic features of the entire ridge is this 19-km-long, very straight, southwestern termination of the northern ridge segment near Jonesboro (fig. 1).

Seismicity in the Crowley's Ridge area is very low. However, diffuse seismicity northeast of the ridge may be associated with the bounding faults on the west side of the rift (Howe, 1985). These same faults pass beneath the ridge near Jonesboro (fig. 3).

DATA ACQUISITION AND PROCESSING

Five Mini-Sosie seismic reflection profiles were recorded across margins of Crowley's Ridge at five different locations (fig. 1). The field data were acquired using common-midpoint seismic reflection techniques (Mayne, 1962). Line lengths varied from 1.5 km at line 4 to 5 km at line 5. Acquisition parameters are listed in table 1.

The Mini-Sosie system is a high-resolution, shallow-reflection seismic technique that uses multiple impacts from gasoline-powered earth tampers (Wackers) as a pseudo-random seismic source (Barbier and others, 1976). The impact moments from each Wacker are identified by a sensor attached to the base plate and sent by radio (carried on the tamper operator's backpack) as a time-break sequence in real time to the Input/Output DHR 2400 seismograph. For each station, three Wackers operated simultaneously and advanced as a tight group along the line of the survey, generating 2,000 impulses. The seismograph correlates the time-break sequence in real time with the seismic signal received by the linear array of geophones to produce a 1-s seismic record from the 2,000 impacts. Source and geophone spacing were selected to image the upper 1 s of two-way travel time (1.2 km) so that the Cretaceous-through-Tertiary section would be recorded. In most of the lines, the top of the Paleozoic was also clearly imaged. This configuration allowed determination of displacement at the top of the Cretaceous and provided resolution to as shallow as 0.15 s (150 m). In
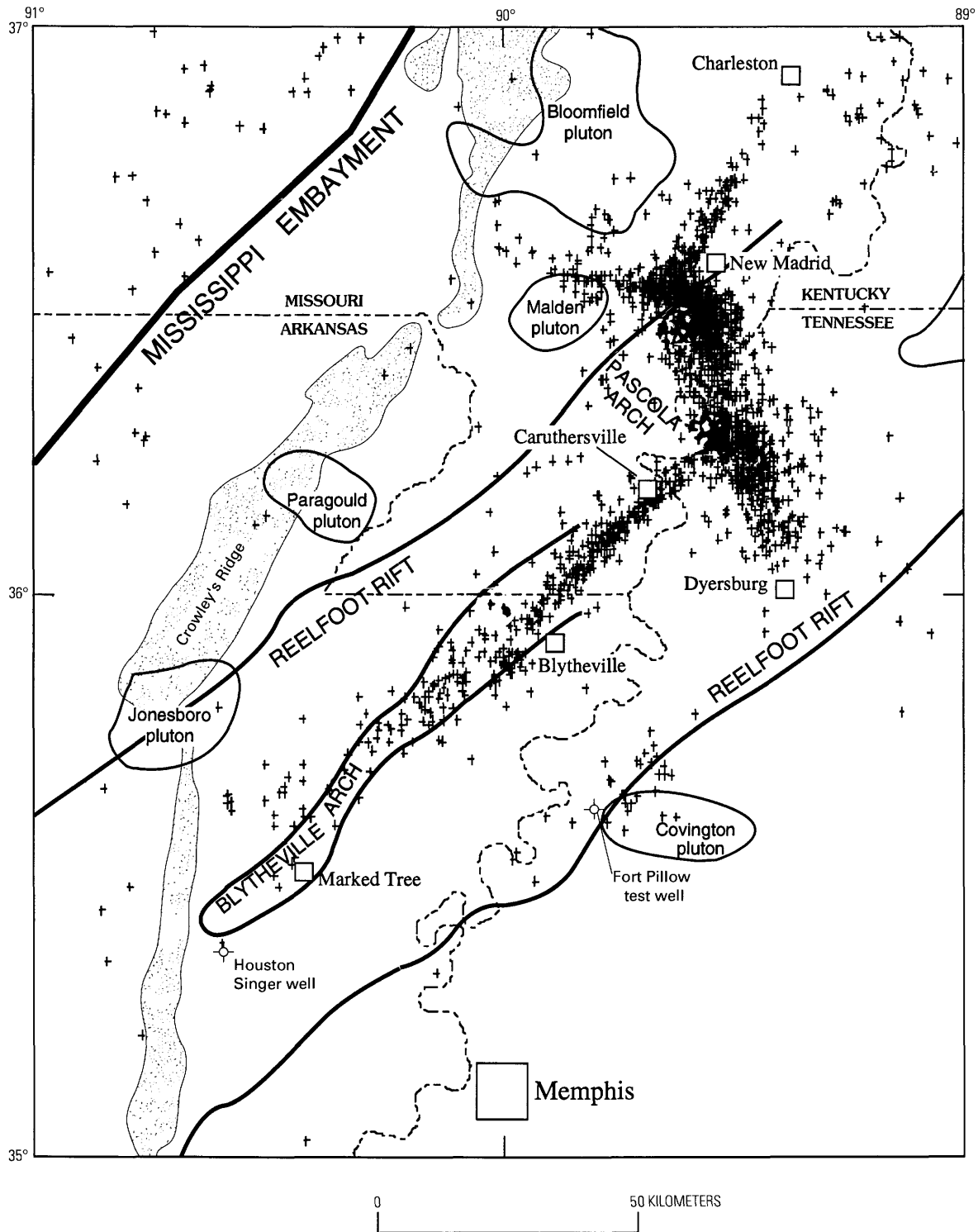
Figure 3. Map showing Crowley's Ridge and epicenters of microearthquakes (+) in the upper Mississippi Embayment (modified from Luzietti and others, 1992).

figures 4–8, the deepest portions of the seismic lines are not reproduced because there are no continuous reflectors in the data.

The surface material along the lines varied from sand-gravel roads (lines 1, 2, and 5) to sand-silt shoulders of paved roads (lines 3 and 4). These variations in surface material may have affected seismic data quality because the data acquired on the sand-gravel roads tends to have more reflection energy, possibly because the elevated shoulders along the paved roads absorb more energy than the hard-pack

Table 1. Data-acquisition parameters and data-processing sequence.

Data-acquisition parameters
Source type:.................3 earth tampers (Wackers)
Source array:................3-m spacing parallel to profile line
Impacts per station:......2,000
Source point interval:...15.2 m (50 ft)
Geophone array:..........12, 28-Hz natural-frequency geophones in a cluster
Geophone spacing:.......15.2 m (50 ft)
Spread geometry:........24 channels, in-line, off-end; ch 1: 30.5-m offset– ch 24: 381-m offset
Recording pass band:..20–240 Hz; 60-Hz notch filter
Recording system:.......I/O DHR 2400, 24-channel Mini-Sosie
Sampling interval: ......1 ms
Record length: ....1 s

Data-processing sequence	
1.	Trace edit
2.	Common midpoint sort
3.	Elevation static timing corrections
4.	Surface-wave surgical mute
5.	Normal moveout velocity correction
6.	Band-pass frequency filter (roughly 30-40-120-150 Hz)
7.	Surface-consistent automatic statics
8.	Refraction mute
9.	Stack (nominally 12-fold)
10.	F-K filter[1]
11.	2nd zero-crossing predictive deconvolution filter
12.	Band-pass frequency filter
13.	Automatic gain control amplitude scaling

[1] Post-stack frequency-wave number.

Table 2. Elevations of geologic units.

[Elevations in meters; minus sign indicates elevation below sea level. Well identification: t, Tennark R.M. Martin and others; q, Quintin Little No. 1 Little; n, J.F. Scott Trustees No. 2-A Nelson]

Sosie line or well	Top of Wilcox Gp.	Top of Midway Gp.	Top of Cretaceous	Top of Paleozoic
1	–180	–231	–685	–823
2	–142	–206	–601	–778
3	–85	–156	–368	–508
4		–8	–268	–375
5	–30	–75	–297	–410
t	–30	–98	–262	–404
q			–276	–421
n				–594

gravel roads. Tests using various geophone group arrays did not significantly alter the signal from a well-developed surface wave enough to warrant the extra time required to handle spreadout geophone arrays. Interference from overhead power lines and other unknown sources of electrical noise required use of a 60-Hz notch filter on all lines. These acquisition parameters resulted in dominant reflection frequencies of about 50 Hz. Despite the attempts to improve data quality using the parameters described above, the overall signal-to-noise (S/N) ratio is quite low (except for line 5) for these data. Evidently, a high water table and compact sands and clays along the fluvial-terrace portions of the lines resulted in relatively good continuity and resolution of reflectors compared to the portions of the lines on Crowley's Ridge where a lower water table and unconsolidated gravel resulted in poorer source and geophone coupling and, therefore, poorer resolution of reflectors beneath the ridge.

The processing parameters are summarized in table 1. Field data were processed on a VAX 780 computer using Digicon's DISCO software at the U.S. Geological Survey facilities in Denver, Colo. The processing flow was relatively standard except for a surgical mute applied prior to

normal-moveout-velocity correction that deleted all data arriving at or below the speed of the surface wave. This mute greatly improved the data S/N ratio, although it also lowered the fold coverage to about 6 or 8 below 0.5 s.

Elevation static corrections were applied using a velocity calculated from refraction energy on near-offset traces displayed in common-shot gathers. These static corrections resulted in a zero time for these profiles that corresponds topographically to the lowest elevation point on each profile. Stacking velocities were determined from common-midpoint gathers and generally ranged from about 1,600 m/s from 0.0 to 0.2 s to 2,000 m/s at 0.7 s. We have good velocity control on lines 2 and 5 (±5 percent), and similar velocity profiles were determined for lines 1, 3, and 4. A post-stack frequency-wave number (F-K) filter also improved the data by removing much of the remaining, dipping, coherent energy not removed by the surgical mute. Because of the generally low S/N ratio on lines 1, 2, 3, and 4, only line 5 was migrated using a post-stack finite-differenced algorithm.

The stratigraphy of the area is detailed in figure 2. Stratigraphic interpretation of the Mini-Sosie lines was undertaken using petroleum test wells located on or near Crowley's Ridge (fig. 1) (Renfroe, 1949; Dart, 1990). Additional data used in interpreting the seismic lines include the New Madrid test well 1-X in New Madrid County, Missouri (Crone, 1981; Frederiksen and others, 1982), the Fort Pillow test well in Lauderdale County, Tennessee (Moore and Brown, 1969), and published seismic lines that pass over (Nelson and Zhang, 1991) or near Crowley's Ridge (Hamilton and Zoback, 1982; Howe and Thompson, 1984; Howe, 1985; Luzietti and others, 1992). As shown in table 2, the elevations of tops of the Eocene Wilcox Group (base of Wilcox may be Paleocene, e.g., Frederiksen and others, 1982), Paleocene Midway Group, Cretaceous section, and Paleozoic section have been picked (Renfroe, 1949) from the Tennark well, located southwest of Jonesboro near the middle of our five lines (fig. 1). Strong reflectors exist at or near the tops of these stratigraphic units in all five seismic lines (table 2 and figs. 4–8).

INTERPRETATION OF MINI-SOSIE REFLECTION LINES

Seismic signatures of the geologic units identified in figures 4–8 are consistent from line to line. The Claiborne Group has discontinuous reflectors; the Wilcox Group has continuous reflectors; the Midway Group has almost no reflectors; the Cretaceous section has continuous reflectors; and the Paleozoic section changes from discontinuous reflectors to no reflectors with depth. The major difference among the five lines is that the reflectors are deeper in lines 1 and 2 because lines 1 and 2 are closer to the Mississippi-Embayment axis.

MINI-SOSIE LINE 1

Line 1 is a 2-km-long line on the western side of the southern ridge segment (figs. 1 and 4). As shown in the topographic profile (fig. 4), the ridge is approximately 30 m high at this location. Line 1 coincides with a portion of the Reelfoot rift COCORP AR-6 line. Although resolution of the top of the Paleozoic is poor in line 1, we believe that it is at 0.8 s at the western end of the line, which corresponds with the 0.8 s time for the top of the Paleozoic in the COCORP line (Nelson and Zhang, 1991). The COCORP line also reveals a near-vertical fault that displaces the Paleozoic Knox through Tertiary sections down to the west beneath the western margin of the ridge (Nelson and Zhang, 1991).

The Wilcox is flat-lying beneath the ridge from station numbers (STAT) 104 to 180. At STAT 180, the Wilcox is displaced approximately 0.04 s (42 m) down to the west and dips gently westward from STAT 180 to the western end of the line. Although not as evident, it appears that the Cretaceous is also displaced 0.03 s (42 m) down to the west at STAT 180. Within the Claiborne, the fault is manifested as truncated reflectors and relatively steep westerly dipping reflectors from STAT 175 to 180. This steep fault can be traced to within 0.15 s (90 m) of the surface, above which there are no reflection data (fig. 4). The fault is located directly beneath the topographic base of Crowley's Ridge and appears to correspond with the fault identified on the COCORP line. Lack of surface strata exposure did not allow us to determine if the fault cuts to the ground surface.

The Nelson No. 2 well is believed to have been drilled near the western end of line 1 (fig. 1 and table 2). However, this well was drilled in 1921, and its exact location is not known. In comparing the depth of the top of the Paleozoic in the well with the calculated depth from line 1, it is apparent that the Paleozoic is 229 m deeper in line 1. If the Nelson No. 2 well is indeed near the western end of line 1, then our calculated depths would be too deep for line 1, or alternatively, there may be a down-to-the-east fault between the well and the seismic line.

MINI-SOSIE LINE 2

Line 2 is a 2-km-long line that descends eastward off Crowley's Ridge, which is 30 m high at this location (fig. 5). Coincident with line 2 is a portion of the Reelfoot rift COCORP line (Nelson and Zhang, 1991). The top of the Paleozoic is at 0.77 s in the eastern end of line 2 and approximately 0.8 s in the COCORP line.

The tops and bases of the Wilcox and Cretaceous sections are well imaged over most of the profile. From STAT 345 to 375, Paleozoic strata through Eocene Wilcox Group strata have been folded and faulted into an anticline with approximately 0.025 s (38 m) of structural relief at the top of the Cretaceous. This structure appears to persist through to the top of the Wilcox. Upturned Wilcox strata from STAT 350 to 375 appear to be truncated by an overlying reflector, which may be an unconformity near the top of the Wilcox. Within the anticline, at STAT 375, a steep west-dipping normal fault displaces the Wilcox 0.02 s (24 m). Also within the anticline, an east-dipping fault has been interpreted at STAT 355 primarily on the evidence of the upturned Wilcox reflectors east of the fault and the upturned Cretaceous reflectors on the west side of the fault. The elevations of the mapped units are the same at the eastern and western ends of the seismic line. Thus, there is no net vertical displacement across this structure. The structure appears to be a transpressional strike-slip fault whose anticlinal core later subsided.

In the deep section, a west-dipping reverse fault at STAT 390 displaces the top of the Cretaceous by approximately 0.02 s (30 m).

At STAT 370, a west-dipping reverse fault displaces Claiborne strata by 0.01 s (7 m). Reflectors within the Claiborne from STAT 345 to 355 dip steeply to the west over the underlying west-sloping unconformity. This steep dip above the unconformity may be depositional dip, but we believe the high declivity suggests post-Claiborne reactivation of the underlying structure.

The faulting and folding in line 2 lie directly beneath the eastern margin of Crowley's Ridge.

MINI-SOSIE LINE 3

Line 3 is oriented north to south and was located across the southwest termination of the northern ridge segment (figs. 1 and 6). A data gap exists between STAT 565 and 575 where the line crosses a highway. The line is 2 km long and the ridge is 40 m high at this location. The Tennark well (fig. 1) is located on top of the ridge, 3.2 km north of line 3. Comparison of elevations of the stratigraphic units reveals that the Paleozoic and Cretaceous tops are 100 m higher and the Midway and Wilcox tops are 50 m higher in the Tennark well that is located on top of the ridge than in the southern end of line 3, which is south of the ridge (table 2). The data in table 2 also reveal that the Midway Group is approximately 50 m thicker in line 3 than in the Tennark well.
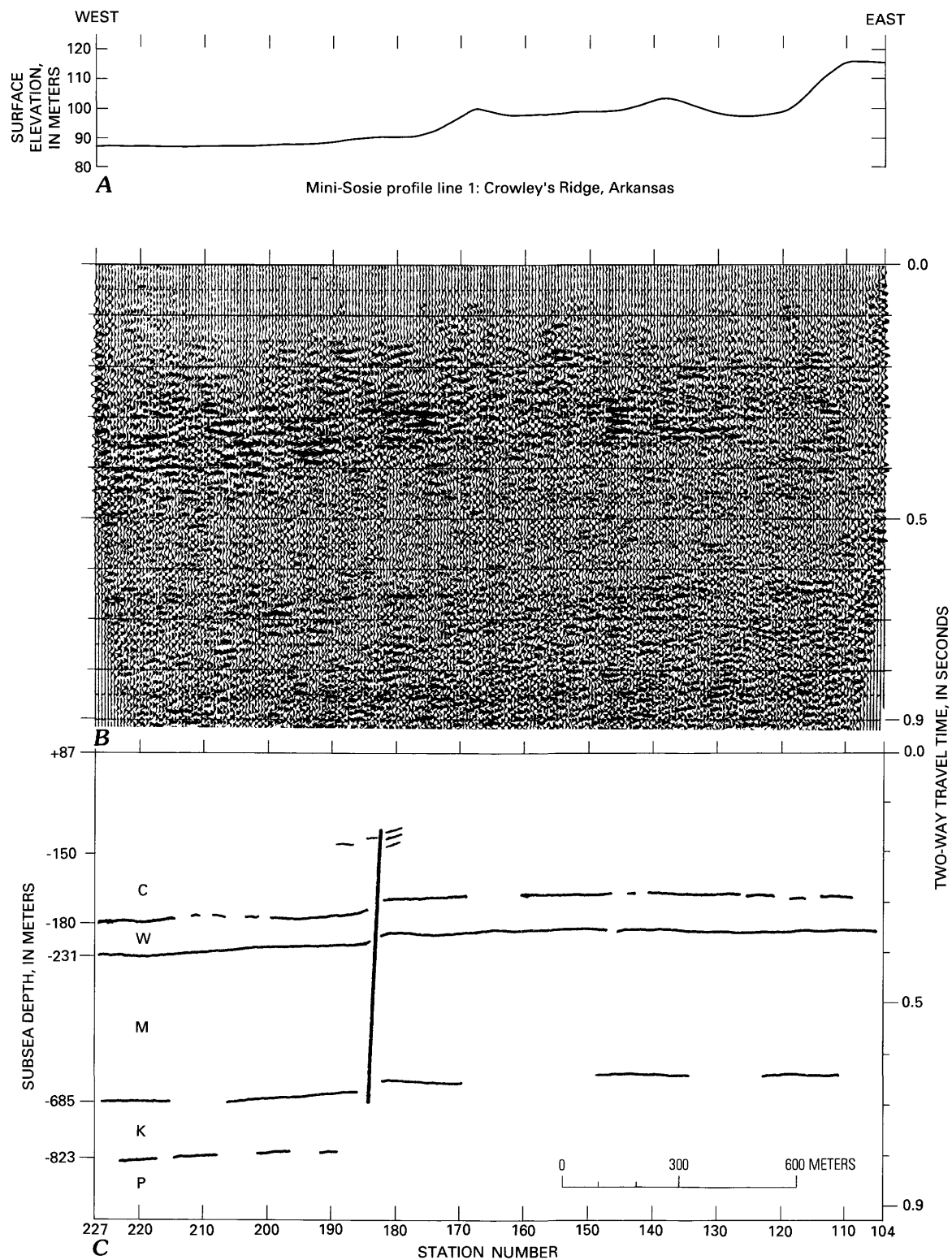
Figure 4. Mini-Sosie line 1: *A*, topographic profile; *B*, reflection profile; *C*, line drawing. See figure 1 for location. The topographic profile has a 7× vertical exaggeration. P, Paleozoic; K, Cretaceous; M, Paleocene Midway Group; W, Eocene Wilcox Group; C, Eocene Claiborne Group.

Figure 5. Mini-Sosie line 2: *A*, topographic profile; *B*, reflection profile, *C*, line drawing. See figure 1 for location. The topographic profile has a 7× vertical exaggeration. P, Paleozoic; K, Cretaceous; M, Paleocene Midway Group; W, Eocene Wilcox Group; C, Eocene Claiborne Group.
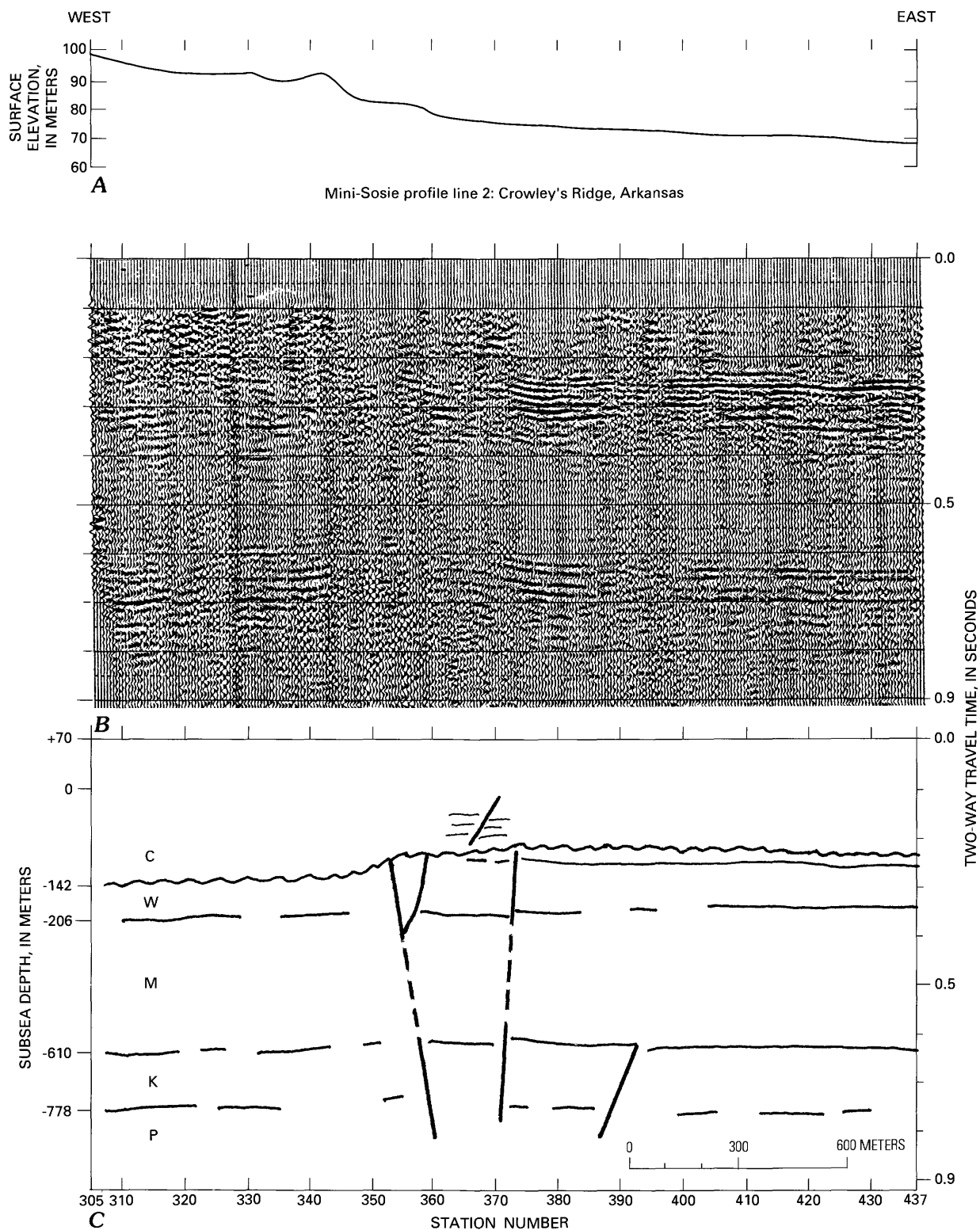
Figure 6. Mini-Sosie line 3: *A*, topographic profile; *B*, reflection profile; *C*, line drawing. See figure 1 for location. The topographic profile has a 5× vertical exaggeration. P, Paleozoic; K, Cretaceous; M, Paleocene Midway Group; W, Eocene Wilcox Group; C, Eocene Claiborne Group.
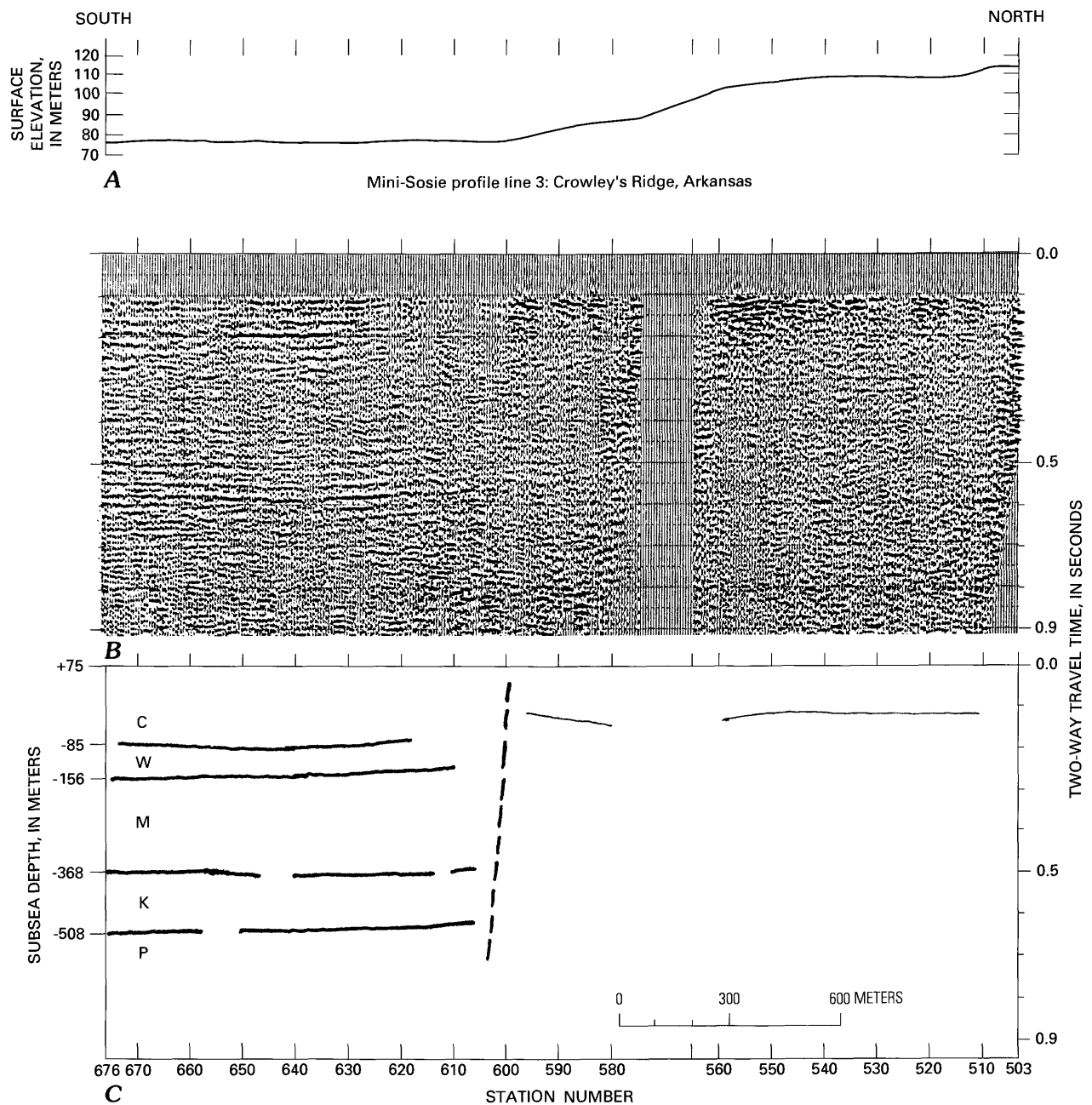
Very few reflectors were imaged beneath the ridge from STAT 503 to 600; however, reflection characteristics from 0.1 to 0.15 s are similar to the Claiborne in the southern portion of the line. Although reflection continuity is poor, it does appear that the upper 0.15 s of reflectors dip north from STAT 600 to 580. Reflectors south of the ridge are continuous and identifiable. From STAT 600 to 635, the reflectors dip southerly, descending 0.02 s (16 m); from STAT 635, they remain horizontal to the southern end of the line.

Perhaps most striking about this line is the absence of Wilcox or lower reflectors north of STAT 600 beneath the ridge. Reflectors can be traced beneath Crowley's Ridge at the other four Mini-Sosie sites; however, apparently local geologic conditions do not permit imaging of strata beneath the ridge at this location with the field and processing methods used in this study.

The upturned and truncated reflectors suggest that a fault lies beneath STAT 600 at the base of Crowley's Ridge.

We believe that either this seismic line has crossed a northwest-trending ridge-bounding fault or the line has intersected, at a low angle, one of the northeast-trending margin faults of the Reelfoot rift (fig. 1). In either case, faulting at this location appears to have occurred both during Midway deposition, because the Midway is thicker in seismic line 3 than in the Tennark well, and after Wilcox deposition.

MINI-SOSIE LINE 4

Line 4 is a 1.5-km-long line located on the west side of the northern segment of Crowley's Ridge (figs. 1 and 7). Topographic relief at this location is 20 m, with three small ridges paralleling the margin of Crowley's Ridge. There are no wells near line 4; however, the calculated elevations of the Paleozoic and Cretaceous in line 4 are reasonably close to those in line 5 and in the Quintin Little and Tennark wells.

All the reflectors dip gently to the east, with five faults displacing the top of the Cretaceous and two of the five displacing the base of the Wilcox. The fault at STAT 715 displaces the Cretaceous 0.06 s (61 m) down to the west. Reflectors are displaced in the Midway Group, but the base of the Wilcox is not disrupted above this fault. At STAT 730, a second fault displaces the Cretaceous 0.015 s (22 m) and basal Wilcox down to the west. The fault at STAT 755 also displaces the Cretaceous 0.02 s (30 m) and basal Wilcox down to the west. A small, west-dipping fault at STAT 770 displaces the Cretaceous 0.01 s (12.5 m). The fault at STAT 785 is a west-dipping fault with 0.01 s (12.5 m) of displacement. The net vertical separation across the entire fault zone is less than the sum of the fault displacements because the strata dip eastward.

There are two, perhaps three, faulting events revealed in line 4. The faulting at STAT 715 occurred during Paleocene Midway deposition but ceased before Wilcox deposition. This down-to-the-west normal faulting resulted in a thicker Midway section west of the fault. Normal faulting also occurred post lower Wilcox, as indicated by the displaced basal Wilcox at STAT 730 and 755. A possible compressional third faulting event is indicated by the small reverse fault at STAT 785. Absence of continuous reflectors in the overlying Midway Group at STAT 785 does not allow us to determine if the Midway Group has also been faulted, and so the timing of this event is indeterminable.

MINI-SOSIE LINE 5

Line 5 is a 5-km-long line located on the east side of the northern segment of Crowley's Ridge (figs. 1 and 8). The data gap between STAT 225 and 235 is where a highway and railroad track were crossed. Ridge topography is subdued in

this area, and the relief of the ridge is 15 m. The western portion of the profile was shot along a gravel road that followed a stream valley, so there is no sharp topographic break at the ridge margin located at STAT 240. Quality of the data in line 5 is excellent with good continuity of reflectors beneath the ridge. The Quintin Little well is located approximately 2.5 km north of the western end of line 5, and the Tennark well is located approximately 15 km southwest of line 5 (fig. 1). As illustrated in table 2, the elevations of the tops of the stratigraphic units in the wells are reasonably close to the calculated depths in line 5. However, we are uncertain whether the uppermost picked reflector is truly the top of the Wilcox or just a strong reflector near the top of the Wilcox.

From STAT 125 to 185, a broad anticline with 0.02 s (25 m) of amplitude is present in the Paleozoic and Cretaceous sections. The fold cannot be identified in the Midway Group, but a much shorter wavelength fold with 0.02 s (14 m) of amplitude occurs in the Wilcox and Claiborne from STAT 150 to 175. When reflectors are projected into the data gap at STAT 230 from the east and west, there appears to be a down-to-the-east fault that displaces the Paleozoic through Wilcox by 0.04 s (56 m). This proposed fault lies beneath the ridge margin. A small horst with 0.01 s (9 m) of displacement is present between STAT 330 and 345. The fault that bounds the west side of the horst appears to fold strata as stratigraphically high as the top of the Wilcox.

A graben is clearly evident at the level of the Paleozoic and Cretaceous sections between STAT 380 and 415. The west bounding fault of the graben displaces the Paleozoic and Cretaceous sections 0.07 s (90 m). Normal-fault displacement of 0.035 s (28 m) at the base of the Wilcox and thickening of the Wilcox indicates that the fault was active during basal Wilcox deposition. The faulting can be traced to the top of the Wilcox, where it appears that there has been reverse movement after Wilcox deposition. This fault comes to within 0.1 s (75 m) of the ground surface and appears to be truncated by flat-lying Claiborne, but better resolution of the uppermost 0.2 s is necessary to determine if faulting reaches the surface. A shallow, antithetic, normal fault at STAT 390 displaces the Wilcox and Claiborne down to the west. The east bounding fault of the deep graben at STAT 420 has 0.025 s (40 m) of displacement at the top of the Cretaceous section, and there is no evidence that this fault displaces overlying Tertiary sediments.

Strata from the western end of the line to STAT 380 are gently easterly dipping to horizontal except adjacent to the structures discussed above. From STAT 380 to the eastern end of the line, the Claiborne and Wilcox dip westerly (opposite to the regional dip) as do the underlying Cretaceous and Paleozoic strata east of the deep graben. Thus, it appears that, during post-Claiborne reactivation of the fault at STAT 380, there was minor westward tilting of the hanging-wall block.
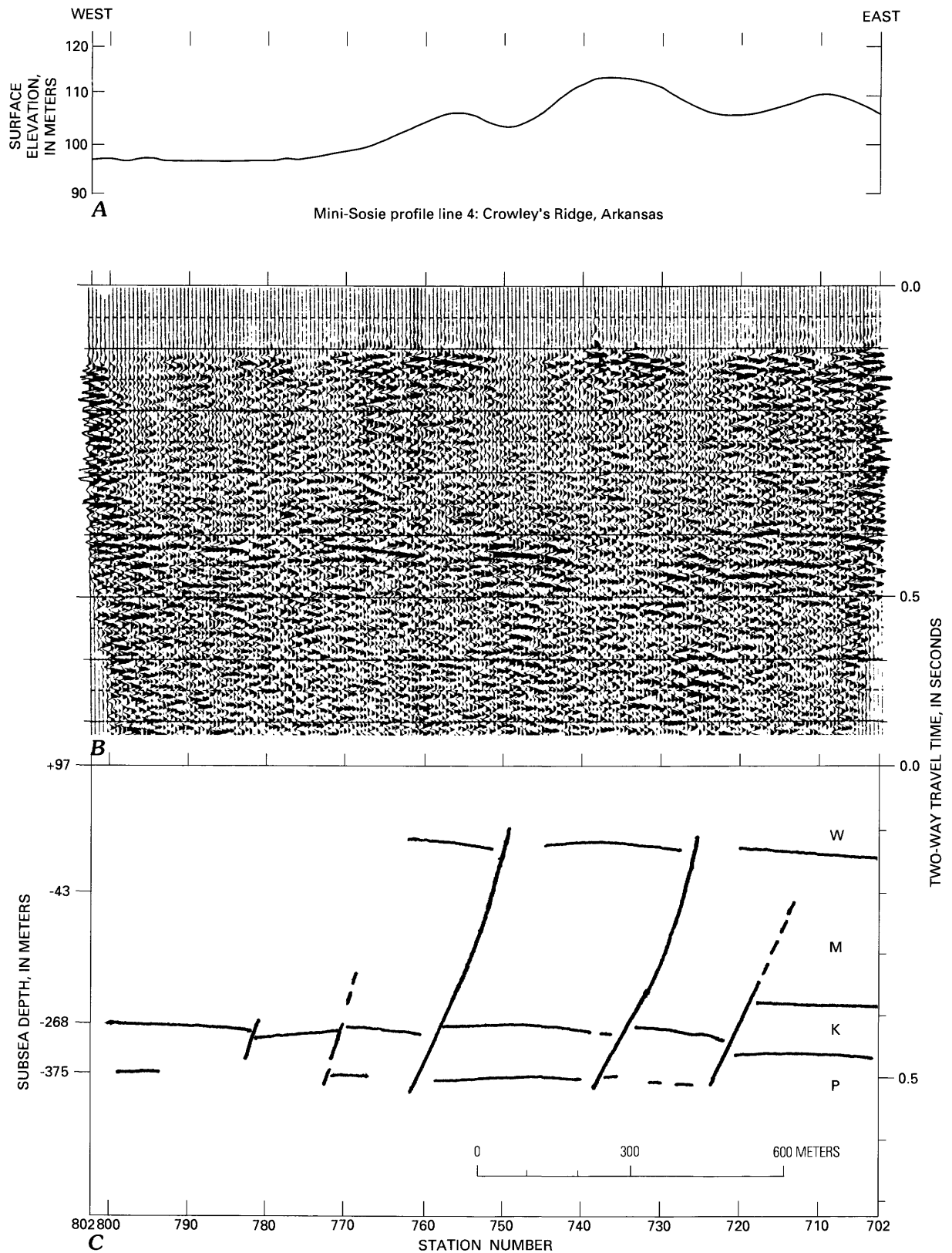
Figure 7. Mini-Sosie line 4: *A*, topographic profile; *B*, reflection profile; *C*, line drawing. See figure 1 for location. The topographic profile has a 10× vertical exaggeration. P, Paleozoic; K, Cretaceous; M, Paleocene Midway Group; W, Eocene Wilcox Group.

Figure 8. Mini-Sosie line 5: A, topographic profile; B, reflection profile; C, line drawing. See figure 1 for location. The topographic profile has a 5× vertical exaggeration. P, Paleozoic; K, Cretaceous; M, Paleocene Midway Group; W, Eocene Wilcox Group.
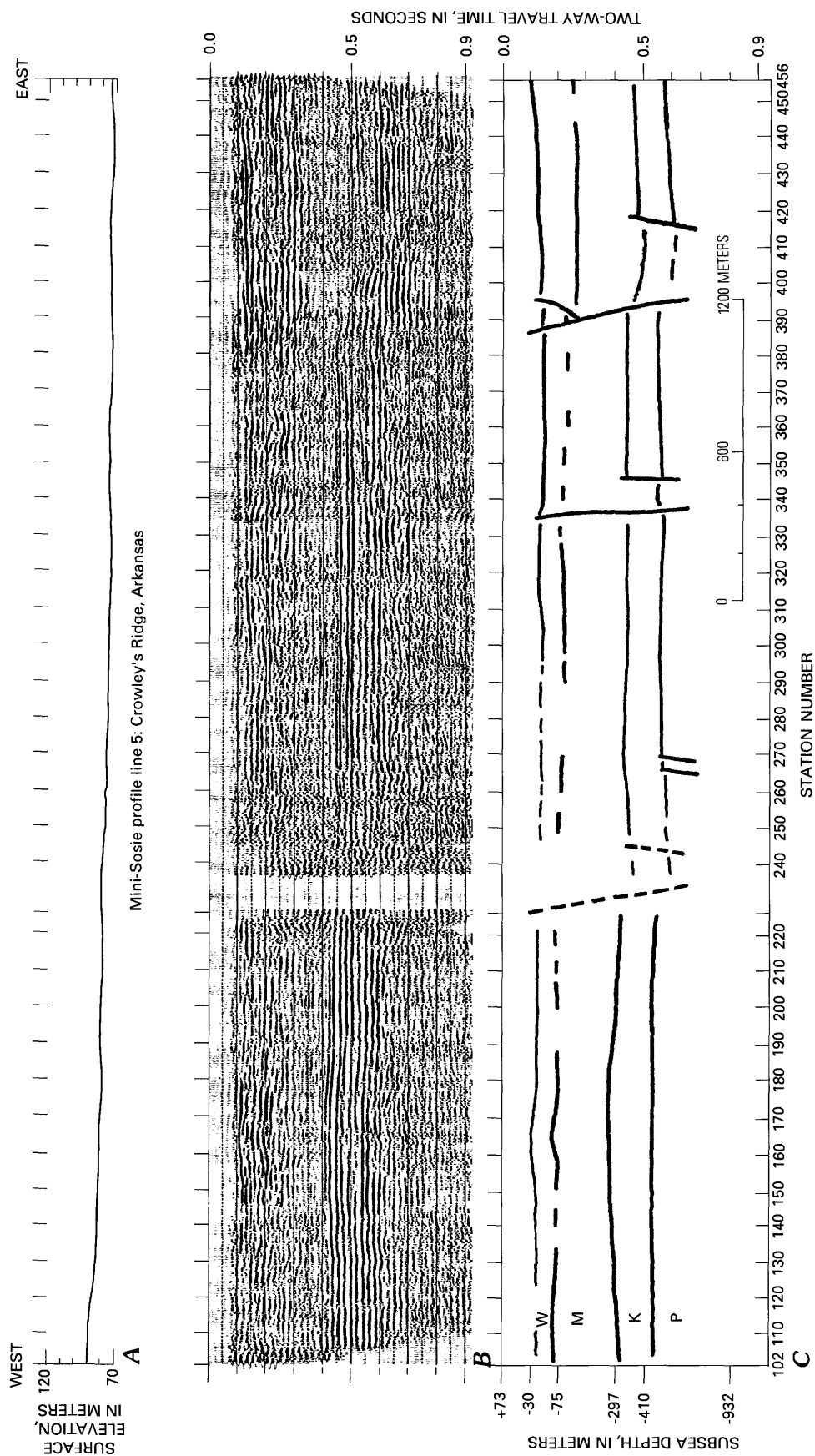
SIMILARITIES BETWEEN CROWLEY'S RIDGE AND THE NEW MADRID SEISMIC ZONE

A comparison of the shape and dimensions of Crowley's Ridge and earthquake epicenter distribution in the New Madrid seismic zone reveals striking similarities (fig. 3). The southern portion of Crowley's Ridge is similar to the southern arm of seismicity (Blytheville arch); the left step of Crowley's Ridge at Jonesboro is similar to the northwest-trending zone of seismicity (Pascola arch and overlying Lake County uplift); and the northern segment of Crowley's Ridge is similar to the northeast-trending northwestern arm of New Madrid seismicity. In addition, the Reelfoot rift margin passes beneath both structures where major changes in orientation occur.

Focal mechanisms along the southern arm of New Madrid seismicity reveal right-lateral strike-slip faulting within the Blytheville arch (Herrmann and Canas, 1978; Stauder, 1982). Reverse faulting is recorded in the northwest-trending zone of seismicity within the Pascola arch, and right-lateral faulting is predominant in the northwestern zone of New Madrid seismicity. Like the New Madrid seismic zone, we believe that the bounding faults of the northern and southern segments of Crowley's Ridge may be strike-slip faults and that the bend at Jonesboro may be a left-stepping bend, perhaps with an underlying reverse fault.

The Mini-Sosie lines suggest that much of the faulting along Crowley's Ridge may be of Paleocene and Eocene age. We believe that Crowley's Ridge may primarily be a Tertiary structure and that current seismicity may now include, or has shifted to, the New Madrid seismic zone. Although most of the faulting of Crowley's Ridge may be Tertiary in age, it is important to note that the faults bounding the ridge are favorably oriented for strike-slip and reverse movement in the current Midcontinent stress field (Zoback and Zoback, 1989).

DISCUSSION AND CONCLUSIONS

A rather complex Tertiary structural history is revealed in the Mini-Sosie lines of Crowley's Ridge. Paleocene normal faulting is evident by the thickening of the Midway Group in line 4. Eocene normal faulting is also revealed by thickening of the Wilcox Group in line 5. Post-Wilcox (early Eocene) normal faulting is evident in all of the lines. The faulted anticline and post-Wilcox erosion in line 2 suggests that the area of line 2 was subjected to transpression and was subaerially exposed just after early Eocene Wilcox time. Post-Claiborne compression is evident in lines 2 and 5, and post-Claiborne normal faulting appears to have occurred in lines 1, 3, and 5.

The steepness of the faults, the normal and reverse-fault movements that occur within a small area and over a relatively short length of time (Paleocene and Eocene), and the marked strike-slip appearance of the major faults in line 2 suggest that most of these faults may be the upper portions of flower structures as has been suggested for other areas of the Mississippi Embayment (Luzietti and Harding, 1991; Schweig and others, 1992).

At line 1, the ridge height is the same as the structural relief on the ridge-bounding fault, and fault displacement can be traced through the shallowest resolvable reflectors (fig. 4). Thus, at this location, we believe the ridge margin is a fault scarp.

Mini-Sosie line 2 displays folding and faulting beneath the eastern margin of the ridge; however, the elevation of the Paleozoic and Cretaceous sections on both sides of the fold are the same (fig. 5). Ten m of post-Claiborne displacement on the small reverse fault at STAT 370 may have lifted Crowley's Ridge to provide some of the 30 m of local ridge relief.

We believe that the ridge margin at line 3 (fig. 6) is probably a fault line because of the upturned and sharply truncated seismic reflectors beneath the ridge margin, the declivity and linearity of the ridge margin, and the difference in elevations of the stratigraphic units in line 3 as compared to the Tennark well on top of the ridge. In the subsurface, a fault through this area appears to define the southwestern limit of artesian flow from the Upper Cretaceous Nacatoch Sand (Boswell and others, 1965); the fault separates two areas of different crustal thickness (Mooney and others, 1983); and the southeastern projection of the fault defines the southern limit of intense liquefaction in 1811–12 and modern New Madrid seismicity near Marked Tree, Ark. (Cox, 1988a, 1988b).

Line 4 reveals a number of faults near the ridge margin (fig. 7). Of the five lines, this line has the greatest amount of topography, and we propose that this topography may be due to displacement on the underlying faults because the faults appear to project to the surface at the base of each small ridge.

Folding and faulting are revealed in line 5 (fig. 8). Post-Claiborne folding is well expressed in this line in addition to post-Wilcox movement on a large graben at the eastern end of the line. The eastern end of the line intersects the western margin of the Reelfoot rift (fig. 1); thus, we believe that the graben indicates Tertiary reactivation of the west bounding faults of the Reelfoot rift.

Crowley's Ridge has faults beneath its margins at all five Mini-Sosie line locations. Because the seismic surveys did not image the uppermost 0.15 s (150 m), it is not possible to determine if these faults reach the ground surface. Thus, we cannot determine if the ridge truly owes its topographic relief to fault displacement or if Tertiary faulting controlled subsequent Quaternary river incision. However, we do

conclude that Crowley's Ridge is not a simple erosional remnant but is structurally controlled.

The seismic potential of the Crowley's Ridge faults is difficult to assess. Crowley's Ridge is seismically quiet. However, the fact that the faults imaged in this study lie at the base of the ridge margins suggests that they have been active within the Quaternary. We believe it is geomorphically unreasonable to maintain topographic scarps above Tertiary faults, particularly when Crowley's Ridge is made of poorly consolidated sands, clays, and gravel.

Most of the faults identified in this study cut the top of the Paleozoic section and have been traced into the Eocene section. However, until we can determine if these faults displace the overlying Wisconsin terrace (Saucier, 1974; Royall and others, 1991) we cannot ascertain the seismic hazard of these faults (Reiter, 1990). A follow-up study is in progress to seismically image the uppermost 0.2 s above the faults identified in this study to determine if the Pliocene and Pleistocene sections have been faulted.

ACKNOWLEDGMENTS

REFERENCES CITED

Autin, W.J., Burns, S.F., Miller, B.J., Saucier, R.T., and Snead, J.I., 1991, Quaternary geology of the lower Mississippi Valley, *in* Morrison, R.B., ed., Quaternary Nonglacial Geology; Conterminous U.S.: Geological Society of America, Geology of North America, v. K–2, p. 547–582.

Barbier, M.G., Bondon, P., Mellinger, R., and Viallix, J.R., 1976, Mini-Sosie for shallow land seismology: Geophysical Prospecting, v. 24, p. 518–527.

Bickford, M.E., 1988, The formation of continental crust: Part 1. A review of some principles: Part 2. An application to the Proterozoic evolution of southern North America: Geological Society of America Bulletin, v. 100, p. 1375–1391.

Boswell, E.H., Moore, G.K., MacCary, L.M., and others, 1965, Cretaceous aquifers in the Mississippi Embayment: U.S. Geological Survey Professional Paper 448–C, 37 p.

Braile, L.W., Keller, G.R., Hinze, W.J., and Lidiak, E.G., 1982, An ancient rift complex and its relationship to contemporary seismicity in the New Madrid seismic zone: Tectonics, v. 1, p. 225–237.

Buschbach, T.C., and Schwalb, H.R., 1984, Sedimentary geology of the New Madrid seismic zone, *in* Gori, P.L., and Hays,

W.W., eds., Proceedings, Symposium on the New Madrid Earthquakes: U.S. Geological Survey Open-File Report 84–770, p. 64–96.

Call, R.E., 1889, The geology of Crowley's Ridge: Annual report of the Geological Survey of Arkansas, 283 p.

Caplan, W.M., 1954, Subsurface geology and related oil and gas possibilities of northeastern Arkansas: Arkansas Division of Geology, Bulletin 20, 124 p.

Cox, R.T., 1988a, Evidence of Quaternary ground tilting associated with the Reelfoot rift zone, northeast Arkansas: Southeastern Geology, v. 28, no. 4, p. 211–224.

————1988b, Evidence of late Cenozoic activity along the Bolivar-Mansfield tectonic zone, Midcontinent, U.S.A.: Compass, v. 65, no. 4, p. 207–213.

Crone, A.J., 1981, Sample description and stratigraphic correlation of the New Madrid test well 1-W, New Madrid County, Missouri: U.S. Geological Survey Open-File Report 81–426, 26 p.

Crone, A.J., McKeown, F.A., Harding, S.T., Hamilton, R.M., Russ, D.P., and Zoback, M.D., 1985, Structure of the New Madrid seismic source zone in southeastern Missouri and northeastern Arkansas: Geology, v. 13, p. 547–550.

Dart, R.L., 1990, Catalog of drill-hole data from wells in the Paleozoic rocks on the upper Mississippi Embayment: U.S. Geological Survey Open-File Report 90–260, 136 p.

Ervin, C.P., and McGinnis, L.D., 1975, Reelfoot rift: Reactivated precursor to the Mississippi Embayment: Geological Society of America Bulletin, v. 86, p. 1287–1295.

Fisk, H.N., 1944, Geologic investigation of the alluvial valley of the lower Mississippi River: Vicksburg, Mississippi, U.S. Army Corps of Engineers, 78 p.

Frederiksen, N.O., Bybell, L.M., Christopher, R.A., Crone, A.J., Edwards, L.E., Gibson, T.G., Hazel, J.E., Repetski, J.E., Russ, D.P., Smith, C.C., and Ward, L.W., 1982, Biostratigraphy and paleoecology of lower Paleozoic, Upper Cretaceous, and lower Tertiary rocks in U.S. Geological Survey New Madrid test wells, southeastern Missouri: Tulane Studies in Geology and Paleontology, v. 17, no. 2, p. 23–45.

Guccione, M.J., Prior, W.L., and Rutledge, E.M., 1986, The Tertiary and Quaternary geology of Crowley's Ridge; a guidebook: Arkansas Geologic Commission, 39 p.

Hamilton, R.M., and McKeown, F.A., 1988, Structure of the Blytheville arch in the New Madrid seismic zone: Seismological Research Letters, v. 59, p. 117–121.

Hamilton, R.M., and Zoback, M.D., 1982, Tectonic features of the New Madrid seismic zone from seismic reflection profiles, *in* McKeown, F.A., and Pakiser, L.C., eds., Investigations of the New Madrid, Missouri, Earthquake Region: U.S. Geological Survey Professional Paper 1236, p. 54–82.

Herrmann, R.B., and Canas, J.A., 1978, Focal mechanism studies in the New Madrid seismic zone: Bulletin of the Seismological Society of America, v. 68, p. 1095–1102.

Hildenbrand, T.G., 1985, Rift structure of the northern Mississippi Embayment from the analysis of gravity and magnetic data: Journal of Geophysical Research, v. 90, p. 12607–12622.

Hildenbrand, T.G., Kane, M.F., and Hendricks, J.D., 1982, Magnetic basement in the upper Mississippi Embayment region— A preliminary report, *in* McKeown, F.A., and Pakiser, L.C., eds., Investigations of the New Madrid, Missouri, Earthquake Region: U.S. Geological Survey Professional Paper 1236, p. 39–53.

Holbrook, D.F., 1980, Arkansas lignite investigations—A preliminary report: Arkansas Geological Commission, 157 p.

Howe, J.R., 1985, Tectonics, sedimentation, and hydrocarbon potential of the Reelfoot aulacogen: University of Oklahoma, unpub. M.S. thesis, 109 p.

Howe, J.R., and Thompson, T.L., 1984, Tectonics, sedimentation, and hydrocarbon potential of the Reelfoot rift: Oil and Gas Journal, v. 82, p. 179–190.

Johnston, A.C., 1982, A major earthquake zone on the Mississippi: Scientific American, v. 246, no. 4, p. 60–68.

Kane, M.F., Hildenbrand, T.G., and Hendricks, J.D., 1981, Model for the tectonic evolution of the Mississippi Embayment and its contemporary seismicity: Geology, v. 9, p. 563–568.

Krinitzsky, E.L., 1950, Geological investigation of faulting in the lower Mississippi valley: Waterways Experiment Station, Technical Memorandum No. 3–311, 41 p.

Luzietti, E.A., and Harding, S.T., 1991, Reconnaissance seismic reflection surveys in the New Madrid seismic zone, northeast Arkansas and southeast Missouri: U.S. Geological Survey Miscellaneous Field Studies Map MF–2135.

Luzietti, E.A., Kanter, L.R., Schweig, E.S., Shedlock, K.M., and VanArsdale, R.B., 1992, Shallow deformation along the Crittenden County fault zone near the southeast margin of the Reelfoot rift, northeastern Arkansas: Seismological Research Letters, v. 63, no. 3, p. 263–275.

Mayne, H.W., 1962, Common reflection point horizontal data stacking techniques: Geophysics, v. 27, p. 952–965.

McKeown, F.A., Hamilton, R.M., Diehl, S.F., and Glick, E.E., 1990, Diapiric origin of the Blytheville and Pascola arches in the Reelfoot rift, east-central United States: Relation to New Madrid seismicity: Geology, v. 18, p. 1158–1162.

Meissner, C.R., 1984, Stratigraphic framework and distribution of lignite on Crowley's Ridge, Arkansas: Arkansas Geologic Commission Information Circular 28–B, 14 p.

Mooney, W.D., Andrews, M.C., Ginzburg, A., Peters, D.A., and Hamilton, R.M., 1983, Crustal structure of the northern Mississippi Embayment and a comparison with other continental rift zones: Tectonophysics, v. 94, p. 327–348.

Moore, G.K., and Brown, D.L., 1969, Stratigraphy of the Fort Pillow test well, Lauderdale County, Tennessee: Tennessee Division of Geology, Report of Investigations 26, 2 p.

Murray, G.E., 1961, Geology of the Atlantic and Gulf Coastal Province of North America: New York, Harper and Brothers, 692 p.

Nelson, K.D., and Zhang, J., 1991, A COCORP deep reflection profile across the buried Reelfoot rift, south-central United States: Tectonophysics, v. 197, nos. 2–4, p. 271–293.

Nuttli, O.W., 1973, The Mississippi Valley earthquakes of 1811 and 1812: Intensities, ground motions and magnitudes: Bulletin of the Seismological Society of America, v. 63, p. 227–248.

———1982, Damaging earthquakes of the central Mississippi Valley, in McKeown, F.A., and Pakiser, L.C., eds., Investigations of the New Madrid, Missouri, Earthquake Region: U.S. Geological Survey Professional Paper 1236, p. 15–20.

O'Leary, D.W., and Hildenbrand, T.G., 1978, Structural significance of lineament and aeromagnetic patterns in the Mississippi Embayment: Proceedings of the 3rd International Conference on Basement Tectonics, 1978, Durango, Colorado, p. 305–313.

Potter, P.E., 1955, The petrology and origin of the Lafayette Gravel: Journal of Geology, v. 63, no. 1, p. 1–38, no. 2, p. 115–132.

Pryor, W.A., 1960, Cretaceous sedimentation in upper Mississippi Embayment: American Association of Petroleum Geologists Bulletin, v. 44, no. 9, p. 1473–1504.

Reiter, L., 1990, Earthquake hazard analysis—Issues and insights: New York, Columbia University Press, 254 p.

Renfroe, C.A., 1949, Petroleum exploration in eastern Arkansas with selected well logs: Arkansas Resource and Development Commission, Division of Geology Bulletin 14, 159 p.

Royall, P.D., Delcourt, P.A., Delcourt, H.R., 1991, Late Quaternary paleoecology and paleoenvironments of the central Mississippi alluvial valley: Geological Society of America Bulletin, v. 103, no. 2, p. 157–170.

Russ, D.P., 1979, Late Holocene faulting and earthquake recurrence in the Reelfoot Lake area, northwestern Tennessee: Geological Society of America Bulletin, v. 90, Part I, p. 1013–1018.

———1982, Style and significance of surface deformation in the vicinity of New Madrid, Missouri, in McKeown, F.A., and Pakiser, L.C., eds., Investigations of the New Madrid, Missouri, Earthquake Region: U.S. Geological Survey Professional Paper 1236, p. 95–114.

Rutledge, E.M., West, L.T., and Guccione, M.J., 1990, Loess deposits of northeast Arkansas, in Guccione, M.J., and Rutledge, E.M. eds., Field Guide to the Mississippi Alluvial Valley—Northeast Arkansas and Southeast Missouri: Friends of the Pleistocene, South-Central Cell, p. 57–98.

Saucier, R.T., 1974, Quaternary geology of the lower Mississippi valley: Arkansas Archaeological Survey Research Series, v. 6, 26 p.

Schwalb, H.R., 1982, Paleozoic geology of the New Madrid area: U. S. Nuclear Regulatory Report NUREG/CR–2909, 61 p.

Schweig, E., Fan Shen, Kanter, L., Luzietti, E., VanArsdale, R., Shedlock, K., and King, K., 1992, Shallow seismic reflection survey of the Bootheel lineament, southeastern Missouri: Seismological Research Letters, v. 63, no. 3, p. 285–295.

Stauder, W., 1982, Present-day seismicity and identification of active faults in the New Madrid seismic zone, in McKeown, F.A., and Pakiser, L.C., eds., Investigations of the New Madrid, Missouri, Earthquake Region: U.S. Geological Survey Professional Paper 1236, p. 21–30.

Stearns, R.G., 1957, Cretaceous, Paleocene, and lower Eocene geologic history of the northern Mississippi Embayment: Geological Society of America Bulletin, v. 68, p. 1077–1100.

Stearns, R.G., and Marcher, M.V., 1962, Late Cretaceous and subsequent structural development of the northern Mississippi Embayment area: Geological Society of America Bulletin, v. 73, p. 1387–1394.

Stephenson, L.W., and Crider A.F., 1916, Geology and ground waters of northeast Arkansas: U. S. Geological Survey Water-Supply Paper 399, 315 p.

Zoback, M.L., and Zoback, M.D., 1989, Tectonic stress field of the continental United States, in Pakiser, L.C., and Mooney, W.D., eds., Geological Society of America Memoir 172, p. 523–539.